MIT OpenCourseWare
http://ocw.mit.edu

Electromechanical Dynamics

For any use or distribution of this textbook, please cite as follows:

Woodson, Herbert H., and James R. Melcher. *Electromechanical Dynamics*.
3 vols. (Massachusetts Institute of Technology: MIT OpenCourseWare).
http://ocw.mit.edu (accessed MM DD, YYYY). License: Creative Commons
Attribution-NonCommercial-Share Alike

For more information about citing these materials or
our Terms of Use, visit: http://ocw.mit.edu/terms

Chapter 13

ELECTROMECHANICS
OF COMPRESSIBLE,
INVISCID FLUIDS

13.0 INTRODUCTION

In this chapter we introduce the additional law (conservation of energy) and constituent relations necessary to describe mathematically a compressible, inviscid fluid. This more general model is then used to study electromechanical interactions. Attention is focused on the effects of compressibility on the MHD machine analyzed in Chapter 12 and on how magnetic fields can affect the propagation of longitudinal disturbances (sound waves) in a compressible fluid.

13.1 INVISCID, COMPRESSIBLE FLUIDS

Cases of electromechanical coupling with fluids that have appreciable compressibility are found in MHD systems which use ionized gases as working fluids. We have chosen a perfect gas as our model of a compressible fluid. Although alternative models can be used, the principal phenomena that we shall study also occur in systems for which other models are appropriate.

It is a well-known fact that when work is done to compress a gas the temperature increases. This is an indication that the mechanical work of compression has been stored as internal (thermal) energy in the gas. The strong coupling between thermal and mechanical energy in a gas will necessitate the inclusion of the conservation of energy as one of the fundamental equations; and it will also require that we specify thermal and mechanical equations of state as constituent relations for the fluid.

The compressible fluids we deal with will obey the conservation of mass as

derived and discussed in Section 12.1.2. The differential form of the conservation of mass is (12.1.11)

$$\frac{D\rho}{Dt} = -\rho(\nabla \cdot \mathbf{v}), \qquad (13.1.1)$$

where (D/Dt) is the substantial derivative defined in (12.1.5)

$$\frac{D}{Dt} = \frac{\partial}{\partial t} + (\mathbf{v} \cdot \nabla). \qquad (13.1.2)$$

The integral form expressing conservation of mass is (12.1.8)

$$\oint_S (\rho \mathbf{v} \cdot \mathbf{n}) \, da = -\frac{d}{dt} \int_V \rho \, dV. \qquad (13.1.3)$$

The surface S encloses the volume V and $\mathbf{n}$ is the outward-directed unit normal vector.

The derivation of the conservation of momentum (Newton's second law) in Section 12.1.3 was done without assuming that the mass density ρ was constant. Consequently, the resulting equations are equally applicable to compressible fluids. The differential form of the momentum equation is (12.1.14)

$$\rho \frac{D\mathbf{v}}{Dt} = \mathbf{F}, \qquad (13.1.4)$$

where $\mathbf{F}$ is the force density applied to the fluid by all sources—mechanical, gravity, and electrical. The integral form of the momentum equation is (12.1.29)

$$\int_V \frac{\partial(\rho \mathbf{v})}{\partial t} dV + \oint_S \rho \mathbf{v}(\mathbf{v} \cdot \mathbf{n}) \, da = \int_V \mathbf{F} \, dV, \qquad (13.1.5)$$

where the surface S encloses the volume V and $\mathbf{n}$ is the outward-directed unit normal vector.

After deriving the conservation of energy equation for a compressible fluid, we describe the appropriate constituent relations. These equations, along with the conservation of mass, the conservation of momentum, and appropriate boundary conditions, will allow us to solve problems in which there is electromechanical coupling with compressible fluids.

13.1.1 Conservation of Energy

In accounting for the conservation of energy we are concerned only with thermal and mechanical energy storage in a fluid. There will be energy input to the fluid from electromechanical conversion. The Poynting theorem can be written as a separate electromagnetic energy conservation equation; in

this system, however, which is quasi-static electromagnetically, this is unnecessary.

When a fluid is in motion, its kinetic energy density (joules per cubic meter) is $\frac{1}{2}\rho v^2$ and its kinetic energy per unit mass (joules per kilogram) is $\frac{1}{2}v^2$. This kinetic energy represents energy storage in the ordered or average motion of fluid particles. In a gas the particles also have random motion. The kinetic energy stored because of random motion is called thermal or internal energy. The internal energy per unit mass (joules/kilogram) is designated as u. The internal energy, like the velocity $\mathbf{v}$, is an Eulerian variable; thus the internal energy of the fluid in the vicinity of a point is specified by the value of u at that point. The internal energy density (joules per cubic meter) is ρu. The total energy per unit mass (kinetic and thermal) of the fluid at a point is $(u + \frac{1}{2}v^2)$; the energy density at any point in space is $\rho(u + \frac{1}{2}v^2)$.

Consider now a volume V enclosed by the surface S with outward-directed unit normal vector $\mathbf{n}$. The conservation of energy for the fluid within the volume is written

$$\int_V \frac{\partial}{\partial t} \rho(u + \tfrac{1}{2}v^2)\, dV + \oint_S \rho(u + \tfrac{1}{2}v^2)\mathbf{v} \cdot \mathbf{n}\, da = [\text{power input to fluid}].$$

$$(13.1.6)$$

The first term on the left specifies the time rate of increase of energy stored by thermal and kinetic energy in the fluid that occupies the volume V at the instant of time in question. The second term on the left specifies the rate at which thermal and kinetic energy is transported across the surface S and out of the volume V. Thus the left side of (13.1.6) represents the energy that must be supplied by the total power input to the fluid in the volume V. This power input can be supplied by volume force densities, such as those of gravity and of electromagnetic origin, by volume heat generation, such as joule losses (J^2/σ) and viscous losses, by forces due to pressure that do work, and by heat conduction and radiation. An inviscid fluid model is being used, and viscous effects are ignored. Heat conduction and radiation will also be ignored because they have very small effects in practical situations on the electromechanical phenomena to be studied.

Before (13.1.6) can be specified in more detail and before a useful differential form can be obtained it is necessary to use the physical properties of the fluid to describe constituent relations.

13.1.2   Constituent Relations

A homogeneous, isotropic, compressible fluid at rest can sustain no shear stresses. Moreover, an inviscid fluid in motion can sustain no shear stresses.

Consequently, the mechanical stresses transmitted by an inviscid incompressible fluid are always normal and compressive; thus we define a pressure p exactly as we did in Section 12.1.4 with the result that the mechanical stress tensor is (12.1.34)

$$T_{ij}{}^m = -\delta_{ij}p. \tag{13.1.7}$$

The traction applied to a surface whose normal vector is $\mathbf{n}$ (12.1.37) is

$$\boldsymbol{\tau}^m = -p\mathbf{n} \tag{13.1.8}$$

and the mechanical force density (12.1.39) is

$$\mathbf{F}^m = -\nabla p. \tag{13.1.9}$$

We model the compressible fluid as a perfect gas. The mechanical equation of state for a perfect gas is

$$p = \rho RT, \tag{13.1.10}$$

where T is the temperature in degrees Kelvin and R is the gas constant for the particular gas in question with units joules per kilogram-°K. The gas constant R is obtained from the universal gas constant R_g as follows. The universal gas constant is

$$R_g = 8.31 \text{ J/mole-}°\text{K}. \tag{13.1.11}$$

The gas constant R in mks units is obtained from

$$R = \frac{R_g}{M}, \tag{13.1.12}$$

where M is the mass of one mole of the gas in kilograms. This is simply the molecular weight multiplied by 10^{-3}; for example, consider Argon, which has a molecular weight of 39.9. The gas constant for Argon is thus

$$R = \frac{8.31}{39.9 \times 10^{-3}} = 208 \text{ J/kg-}°\text{K}. \tag{13.1.13}$$

Equation 13.1.10 is conventionally called a mechanical equation of state. Because we must consider internal energy storage in the gas, we must also specify a thermal equation of state that relates the internal energy storage to the variables of the system.* For a perfect gas the internal energy is a function of temperature alone and is conventionally expressed as

$$du = c_v \, dT, \tag{13.1.14}$$

where c_v is the specific heat capacity at constant volume with units joules per kilogram-°K. Equation 13.1.14 is expressed in differential form because,

---

* For a more thorough discussion see, for instance, W. P. Allis and M. A. Herlin, *Thermodynamics and Statistical Mechanics*, McGraw-Hill, New York, 1952, pp. 16–20 and 62–65.

over the range of temperatures of interest to us, c_v can be assumed constant; but over a wider range of temperature c_v is not constant and the variation must be accounted for in evaluating internal energy. Our purpose of examining electromechanical interaction phenomena will be served adequately by assuming that the specific heat capacity is constant.

Another specific heat capacity often useful and that we assume is constant in our treatment is the specific heat capacity at constant pressure c_p, which is related to c_v by the expression

$$c_p = c_v + R. \tag{13.1.15}$$

Yet another useful parameter is the ratio of specific heat capacities

$$\gamma = \frac{c_p}{c_v}. \tag{13.1.16}$$

In the ranges of temperature and pressure and for the gases of interest in this treatment the specific heat capacities vary appreciably but the ratio of specific heat capacities remain essentially constant.* Our assumption that all three parameters are constant is adequate for describing the phenomena resulting from electromechanical interactions.

Now that we have described the physical properties of inviscid, compressible fluids by the constituent relations of (13.1.9), (13.1.10), and (13.1.14) we shall recast the momentum and energy equations in more useful forms. We are concerned primarily with pressure and electromagnetic forces and we neglect the force of gravity.

The use of (13.1.9) for the mechanical force density in (13.1.4) yields the momentum equation in the form

$$\rho \frac{D\mathbf{v}}{Dt} = -\nabla p + \mathbf{F}^e, \tag{13.1.17}$$

where $\mathbf{F}^e$ is the force density of electrical origin. To rewrite the integral form of the momentum equation we use

$$\int_V -\nabla p \, dV = \oint_S -p\mathbf{n} \, da \tag{13.1.18}$$

to write (13.1.5) in the form

$$\int_V \frac{\partial(\rho\mathbf{v})}{\partial t} \, dV + \oint_S \rho\mathbf{v}(\mathbf{v} \cdot \mathbf{n}) \, da = \oint_S -p\mathbf{n} \, da + \int_V \mathbf{F}^e \, dV. \tag{13.1.19}$$

* For a thorough discussion of the properties of gases, see, for example, H. B. Callen, *Thermodynamics*, Wiley, New York, 1960, pp. 324–333.

To write the energy equation (13.1.6) in more precise form we must specify the power input to the fluid within the volume V from all sources. Consider first the pressure forces that can be viewed as doing net work only at the surface of the volume V. Thus, because the pressure forces are compressive and normal to any surface, the power input to the fluid from pressure forces is

$$\oint_S -p\mathbf{v} \cdot \mathbf{n} \, da.$$

The use of the divergence theorem allows us to write this quantity as

$$\oint_S -\mathbf{n} \cdot (p\mathbf{v}) \, da = \int_V -\mathbf{\nabla} \cdot (p\mathbf{v}) \, dV. \qquad (13.1.20)$$

The electrical power input to the fluid within the volume V is the total rate at which electrical work is done on charged particles. This includes both the work done by electromagnetic forces and the electrical losses due to finite conductivity in the fluid. In all cases the electrical input power density is $\mathbf{J} \cdot \mathbf{E}$ and the total electrical power input is

$$\begin{bmatrix} \text{electrical power} \\ \text{input} \end{bmatrix} = \int_V \mathbf{J} \cdot \mathbf{E} \, dV. \qquad (13.1.21)$$

To interpret $\mathbf{J} \cdot \mathbf{E}$ as the input power density to the moving gas consider first a *magnetic field system* and denote with primes the variables defined in a reference frame fixed with respect to the fluid. Using (6.1.36), (6.1.37), and (6.1.38)*, we write

$$\mathbf{J} \cdot \mathbf{E} = \mathbf{J}' \cdot (\mathbf{E}' - \mathbf{v} \times \mathbf{B}'). \qquad (13.1.22)$$

Then from the vector identity

$$\mathbf{J}' \cdot \mathbf{v} \times \mathbf{B}' = -\mathbf{J}' \times \mathbf{B}' \cdot \mathbf{v}$$

it follows that

$$\mathbf{J} \cdot \mathbf{E} = \mathbf{J}' \cdot \mathbf{E}' + \mathbf{J}' \times \mathbf{B}' \cdot \mathbf{v}. \qquad (13.1.23)$$

The first term on the right is the electric power density that heats up the fluid. For a linear conductor $\mathbf{J}' = \sigma\mathbf{E}'$ and

$$\mathbf{J}' \cdot \mathbf{E}' = \frac{J'^2}{\sigma}.$$

The second term on the right of (13.1.23) is simply $\mathbf{F}^e \cdot \mathbf{v}$, which is the rate at which the magnetic force density does mechanical work on the fluid.

For an *electric field system* we use (6.1.54), (6.1.56), and (6.1.58)* to write $\mathbf{J} \cdot \mathbf{E}$ in the reference frame of the fluid as

$$\mathbf{J} \cdot \mathbf{E} = (\mathbf{J} + \rho'\mathbf{v}) \cdot \mathbf{E}'. \qquad (13.1.24)$$

* See Table 6.1, Appendix G.

Expansion of this expression yields

$$\mathbf{J} \cdot \mathbf{E} = \mathbf{J}' \cdot \mathbf{E}' + \rho' \mathbf{E}' \cdot \mathbf{v}. \qquad (13.1.25)$$

The first term on the right is the rate of heating of the fluid and the second term is the rate at which the electric force density $\rho' \mathbf{E}'$ does mechanical work on the fluid.

The use of (13.1.20) and (13.1.21) with (13.1.6) yields

$$\int_V \frac{\partial}{\partial t} \left[\rho(u + \tfrac{1}{2}v^2)\right] dV + \oint_S \rho(u + \tfrac{1}{2}v^2)\mathbf{v} \cdot \mathbf{n}\, da$$

$$= \int_V -\nabla \cdot (p\mathbf{v})\, dV + \int_V \mathbf{J} \cdot \mathbf{E}\, dV. \quad (13.1.26)$$

The divergence theorem is used to write

$$\oint_S \rho(u + \tfrac{1}{2}v^2)\mathbf{v} \cdot \mathbf{n}\, da = \int_V \nabla \cdot [\rho(u + \tfrac{1}{2}v^2)\mathbf{v}]\, dV. \qquad (13.1.27)$$

Then all terms in (13.1.26) are volume integrals. The volume is arbitrary; thus the equation must hold for the differential volume dV.

$$\frac{\partial}{\partial t} \left[\rho(u + \tfrac{1}{2}v^2)\right] + \nabla \cdot [\rho(u + \tfrac{1}{2}v^2)\mathbf{v}] = -\nabla \cdot p\mathbf{v} + \mathbf{J} \cdot \mathbf{E}. \quad (13.1.28)$$

Expansion of the derivatives in the two terms on the left and use of the conservation of mass (13.1.1) yield the simplified result

$$\rho \frac{D}{Dt}(u + \tfrac{1}{2}v^2) = -\nabla \cdot (p\mathbf{v}) + \mathbf{J} \cdot \mathbf{E}. \qquad (13.1.29)$$

Equations 13.1.26 and 13.1.29 are convenient forms that express the conservation of energy for time-varying situations. Many important problems involve steady flow, in which case $(\partial/\partial t = 0)$ and (13.1.26) simplifies to

$$\oint_S \rho(u + \tfrac{1}{2}v^2)\mathbf{v} \cdot \mathbf{n}\, da = \int_V -\nabla \cdot (p\mathbf{v})\, dV + \int_V \mathbf{J} \cdot \mathbf{E}\, dV \quad (13.1.30)$$

and (13.1.29) simplifies to

$$\rho(\mathbf{v} \cdot \nabla)(u + \tfrac{1}{2}v^2) = -\nabla \cdot (p\mathbf{v}) + \mathbf{J} \cdot \mathbf{E}. \qquad (13.1.31)$$

This last equation is conventionally written in a different form by expanding the first term on the right

$$\nabla \cdot (p\mathbf{v}) = (\mathbf{v} \cdot \nabla)p + p(\nabla \cdot \mathbf{v}). \qquad (13.1.32)$$

The use of the conservation of mass to eliminate $\nabla \cdot \mathbf{v}$ yields

$$\nabla \cdot (p\mathbf{v}) = (\mathbf{v} \cdot \nabla)p - \frac{p}{\rho}(\mathbf{v} \cdot \nabla)\rho. \tag{13.1.33}$$

Recognizing that

$$(\mathbf{v} \cdot \nabla)\frac{p}{\rho} = \frac{1}{\rho}(\mathbf{v} \cdot \nabla)p - \frac{p}{\rho^2}(\mathbf{v} \cdot \nabla)\rho.$$

We write (13.1.33) in the form

$$\nabla \cdot (p\mathbf{v}) = \rho(\mathbf{v} \cdot \nabla)\frac{p}{\rho}$$

and (13.1.31) becomes

$$\rho(\mathbf{v} \cdot \nabla)\left(u + \frac{p}{\rho} + \tfrac{1}{2}v^2\right) = \mathbf{J} \cdot \mathbf{E}. \tag{13.1.34}$$

This expression is simplified further by defining the *specific enthalpy h* as

$$h = u + \frac{p}{\rho} = u + RT \tag{13.1.35}$$

or, in differential form,

$$dh = du + R\,dT = (c_v + R)\,dT = c_p\,dT. \tag{13.1.36}$$

Thus (13.1.34) is written as

$$\rho(\mathbf{v} \cdot \nabla)(h + \tfrac{1}{2}v^2) = \mathbf{J} \cdot \mathbf{E}. \tag{13.1.37}$$

This equation is in a form that emphasizes the electromechanical aspects of a problem. It shows that electrical input power goes into enthalpy or kinetic energy in the gas. Thus for steady-flow problems enthalpy plays the role of energy storage in the gas other than kinetic energy.

13.2 ELECTROMECHANICAL COUPLING WITH COMPRESSIBLE FLUIDS

Now that we have completed the description of the mathematical models we shall use for inviscid, compressible fluids, we treat some steady-state and dynamic systems that emphasize the physical consequences of electromechanical coupling. The simplest examples that illustrate the electromechanical aspects of the problems are selected. It should be clear that many other effects will be significant in an engineering system that uses the basic phenomena that we describe. The details of these other effects are outside the scope of this work but they are well-documented in the literature.*

* See, for example, G. W. Sutton and A. Sherman, *Engineering Magnetohydrodynamics*, McGraw-Hill, New York, 1965.
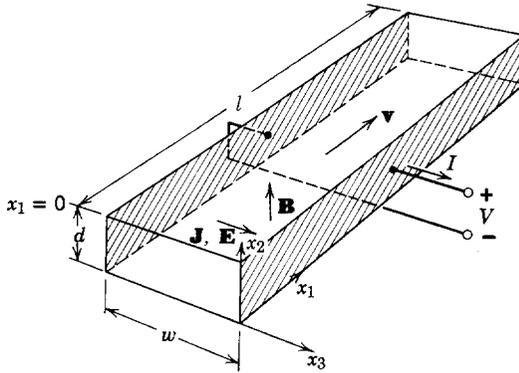
Fig. 13.2.1 A conduction-type MHD machine with constant-area channel.

13.2.1 Coupling with Steady Flow in a Constant-Area Channel

In this section we analyze the system of Fig. 13.2.1 which consists of a channel of constant cross-sectional area through which an electrically conducting gas flows with velocity v. The electrical conductivity is high enough to justify a quasi-static magnetic field model. The two walls perpendicular to the x_2-direction are electrical insulators and the two walls perpendicular to the x_3-direction are highly conducting electrodes. A flux density **B** is produced in the x_2-direction by external means not shown. The electrodes are connected to electrical terminals at which a voltage V and current I are defined. Note that this is the same configuration as that in Fig. 12.2.3 which was used in Section 12.2.1a for the analysis of electomechanical coupling with an inviscid, incompressible fluid. Thus the example in this section, when compared with that of Section 12.2.1a, highlights the effects of compressibility on the basic MHD interaction.

We assume that the l/w and l/d ratios of the channel are large enough that we can reasonably neglect end effects. Also it is assumed that the flow velocity is uniform over the cross section of the channel and that the magnetic field induced by current in the fluid is negligible compared with the applied field (low magnetic Reynolds number). Thus the magnetic flux density and electric field intensity are constant and uniform along the length of the channel

$$\mathbf{B} = \mathbf{i}_2 B_2, \tag{13.2.1}$$

$$\mathbf{E} = \mathbf{i}_3 E_3 = -\mathbf{i}_3 \frac{V}{w}, \tag{13.2.2}$$

and the velocity and current density are given by

$$\mathbf{v} = \mathbf{i}_1 v_1, \tag{13.2.3}$$

$$\mathbf{J} = \mathbf{i}_3 J_3. \tag{13.2.4}$$

The velocity v_1, current density J_3, and the gas variables (p, ρ, T) are functions of x_1 but not of x_2 and x_3. We assume that the gas has a constant, scalar electrical conductivity σ and consider only a steady-flow problem.

The equations that describe this essentially one-dimensional problem are obtained by simplifying equations already presented. From (13.1.1) we obtain the equation for the conservation of mass:

$$v_1 \frac{d\rho}{dx_1} + \rho \frac{dv_1}{dx_1} = 0. \tag{13.2.5}$$

The momentum equation is obtained from (13.1.17) with $\mathbf{F}^e = \mathbf{J} \times \mathbf{B}$:

$$\rho v_1 \frac{dv_1}{dx_1} = -\frac{dp}{dx_1} - J_3 B_2. \tag{13.2.6}$$

The conservation of energy (13.1.37) yields

$$\rho v_1 \frac{d}{dx_1} (h + \tfrac{1}{2}v_1^2) = J_3 E_3. \tag{13.2.7}$$

The mechanical equation of state (13.1.10) is

$$p = \rho R T \tag{13.2.8}$$

and the thermal equation of state (13.1.36) is

$$dh = c_p \, dT. \tag{13.2.9}$$

Finally, Ohm's law for the moving gas is $\mathbf{J}' = \sigma \mathbf{E}'$ or*

$$J_3 = \sigma(E_3 + v_1 B_2). \tag{13.2.10}$$

In these equations a total space derivative is written because x_1 is the only independent variable.

The six equations (13.2.5) to (13.2.10) have six unknowns $(p, \rho, T, h, v_1, J_3)$ that vary with x_1. These equations are nonlinear and direct integration in a general form is not possible. The usual method of solution is to assume that all of the variables are known at the inlet and then to integrate the equations numerically to find the variables along the length of the channel.

The equations can be put in a form convenient for interpretation and numerical integration by finding *influence coefficients*. This process is one of essentially finding each space derivative as a function of the variables themselves. In the derivation of influence coefficients it is convenient to define the velocity of sound (see Section 13.2.3)

$$a = \sqrt{\gamma R T} \tag{13.2.11}$$

* Table 6.1, Appendix G or Section 6.3.1.

and the Mach number of the flow

$$M = \frac{v_1}{a}. \tag{13.2.12}$$

By manipulating (13.2.5) to (13.2.10) and using (13.2.11), (13.2.12), and the ratio of specific heat capacities γ (13.1.16) we obtain the influence coefficients in these forms

$$\frac{1}{v_1}\frac{dv_1}{dx_1} = -\frac{1}{\rho}\frac{d\rho}{dx_1} = \frac{[(\gamma-1)E_3 + \gamma v_1 B_2]J_3}{(1-M^2)\gamma p v_1}, \tag{13.2.13}$$

$$\frac{1}{T}\frac{dT}{dx_1} = \frac{[(1-\gamma M^2)E_3 - \gamma M^2 v_1 B_2](\gamma-1)J_3}{(1-M^2)\gamma p v_1}, \tag{13.2.14}$$

$$\frac{1}{p}\frac{dp}{dx_1} = -\frac{\{(\gamma-1)M^2 E_3 + [1+(\gamma-1)M^2]v_1 B_2\}\gamma J_3}{(1-M^2)\gamma p v_1}, \tag{13.2.15}$$

$$\frac{1}{M^2}\frac{d(M^2)}{dx_1} = \frac{\{(\gamma-1)(1+\gamma M^2)E_3 + \gamma[2-(\gamma-1)M^2]v_1 B_2\}J_3}{(1-M^2)\gamma p v_1}. \tag{13.2.16}$$

We first use these influence coefficients to draw some general conclusions about electromechanical interactions with a conducting gas and then solve a problem in some detail to assess the consequences of compressibility.

First, with reference to Fig. 13.2.1, consider the situation in which the system is acting as a *generator* along the length of the channel. In this case

$$E_3 < 0, \qquad J_3 = \sigma(E_3 + v_1 B_2) > 0.$$

It is clear from (13.2.13) to (13.2.16) that we can distinguish two cases:

$$\text{subsonic flow} \qquad M^2 < 1,$$
$$\text{supersonic flow} \qquad M^2 > 1.$$

For subsonic flow ($M^2 < 1$) (13.2.13) to (13.2.16) yield the results

$$\frac{dv_1}{dx_1} > 0, \qquad \frac{d\rho}{dx_1} < 0, \qquad \frac{dp}{dx_1} < 0, \qquad \frac{dT}{dx_1} < 0, \qquad \frac{d(M^2)}{dx_1} > 0.$$

These results show the curious property that with $\mathbf{J} \times \mathbf{B}$ in a direction to decelerate the gas the flow velocity actually increases. This is a direct result of compressibility. The temperature decreases rapidly enough for the enthalpy of the gas to supply both the energy fed into the electrical circuit and the energy necessary for the increasing kinetic energy.

For supersonic flow ($M^2 > 1$) (13.2.13) to (13.2.16) yield the results

$$\frac{dv_1}{dx_1} < 0, \qquad \frac{d\rho}{dx_1} > 0, \qquad \frac{dp}{dx_1} > 0, \qquad \frac{dT}{dx_1} > 0, \qquad \frac{d(M^2)}{dx_1} < 0.$$

In this case the fluid decelerates as would at first be expected because the $\mathbf{J} \times \mathbf{B}$ force density tends to decelerate the gas. At the same time, however, the increase in temperature indicates that the kinetic energy of the gas supplies both the electrical output power and the power necessary to increase the enthalpy of the gas.

In the subsonic case the Mach number increases and in the supersonic case it decreases. Both changes make the Mach number tend toward unity. It is clear from (13.2.13) to (13.2.16) that the derivatives go to infinity at $M^2 = 1$ and our model becomes inaccurate. The treatment of the flow in the vicinity of the Mach number of one is outside the scope of our discussion. Suffice it to say that for a subsonic flow that approaches Mach one the flow chokes, and a smooth transition to supersonic flow is possible only for a very special set of circumstances. For a supersonic flow that approaches Mach one a shock wave will form. A shock wave is a narrow region in which the gas variables change rapidly and the flow velocity changes from supersonic to subsonic. A more complete model of the gas than we have used is necessary for an analysis of shock waves. The additional constraint needed is the second law of thermodynamics.*

The operation of the system in Fig. 13.2.1 as a *pump* is somewhat more complicated. By operation as a pump (or accelerator) we mean that the terminal voltage has the polarity shown, and $v_1 > 0$, $J_3 < 0$. Thus electric power is fed into the channel, and the $\mathbf{J} \times \mathbf{B}$ force density is in a direction that tends to accelerate the gas. Whether it does accelerate depends on the results obtained from (13.2.13) to (13.2.16).

Consider first the subsonic flow ($M^2 < 1$). The requirement that $J_3 < 0$ imposes through (13.2.10) the requirement that

$$E_3 < -v_1 B_2.$$

This ensures that electric power will be put into the fluid. Equations 13.2.13 and 13.2.14 yield the qualitative sketches of Fig. 13.2.2a. The constant γ is always in the range $1 < \gamma < 2$; thus we must distinguish two possible curves for the temperature variation. It is evident from Fig. 13.2.2a that a $\mathbf{J} \times \mathbf{B}$ force density applied in a direction that tends to accelerate a gas flowing with subsonic velocity may actually decelerate the flow and heat the gas to a higher temperature. The curve of (dv_1/dx_1) also indicates that when the magnitude of J_3 is made large enough the flow velocity can be increased.

For supersonic flow ($M^2 > 1$) with $J_3 < 0$ and the terminal voltage set to the polarity indicated in Fig. 13.2.1 (13.2.13) and (13.2.14) yield the qualitative curves of Fig. 13.2.1b. The upper curve indicates that for small magnitudes

---

* For a thorough and lucid description of the many fluid-mechanical phenomena that can occur in one-dimensional steady flow see A. H. Shapiro, *The Dynamics and Thermodynamics of Compressible Fluid Flow*, Vol. I, Ronald, New York, 1953, pp. 73–264.
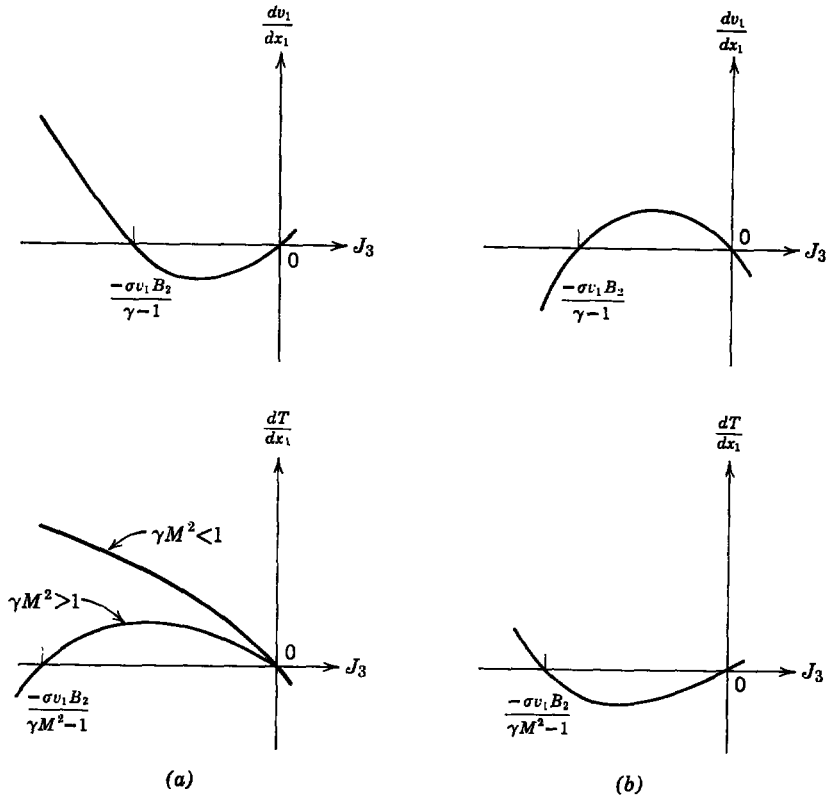
Fig. 13.2.2 Variation of velocity and temperature in a constant-area channel flow of a compressible fluid driven by a J × B force: (a) subsonic ($M^2 < 1$); (b) supersonic ($M^2 > 1$).

of J_3 the velocity is accelerated, but for too much driving current the velocity decreases.

Phenomena such as those demonstrated in Fig. 13.2.2 complicate the behavior of MHD devices that use compressible working fluids. Such phenomena are crucial in applications like plasma propulsion in which the object is to obtain a gas velocity as high as possible. When it is realized that these complications are predicted by an extremely simple model that neglects viscous and boundary layer effects, turbulence, and variation of electrical conductivity with temperature and is not complete enough to describe shock waves in supersonic flow, then we understand how complex the behavior of gaseous MHD systems can be and how we have to be extremely careful in obtaining the desired result from a particular model.

In order to understand how the behavior of a constant-area channel, MHD machine is affected by compressibility and to compare it with the incompressible analysis of Section 12.2.1a, a numerical example is presented.

For this example we assume gas properties typical of seeded combustion gases suitable for use in MHD generators:

$$R = 250 \text{ J/kg}^\circ\text{K}, \qquad \gamma = 1.4, \qquad c_p = 875 \text{ J/kg}^\circ\text{K}, \qquad \sigma = 40 \text{ mhos/m}.$$

We assume that the inlet ($x_1 = 0$) conditions are known:

$$v_1(0) = 500 \text{ m/sec}, \qquad T(0) = 3000^\circ\text{K},$$
$$p(0) = 4 \times 10^5 \text{ N/m}^2, \qquad \rho(0) = 0.534 \text{ kg/m}^3,$$
$$M^2(0) = 0.238.$$

The channel dimensions are assumed to be $w = 0.2$ m, $d = 0.1$ m., and $l = 0.95$ m. The terminals are constrained with a constant voltage source

$$V = 150 \text{ V},$$

which constrains the electric field intensity to be constant along the length of the channel

$$E_3 = -750 \text{ V/m}.$$

The magnetic flux density is assumed to be

$$B_2 = 3 \text{ Wb/m}^2.$$

These numerical values lead to an inlet current density

$$J_3(0) = 3 \times 10^4 \text{ A/m}^2.$$

These numerical data are used with numerical integration of (13.2.13) and (13.2.14) and the mechanical equation of state and the definition of the Mach number to generate the normalized curves of Fig. 13.2.3. It is clear from these curves that the gas properties and flow velocity vary significantly over the length of the channel. Moreover, the rate of variation increases with x_1. With reference to the curve of M^2, it is evident that if the channel were made longer M^2 would pass through unity. Although the equations would give numerical answers, the solutions are physically impossible because the flow would choke and it would be impossible physically to make the Mach number greater than unity.

For this particular generator and these specified conditions the current density can be integrated numerically over the length of the channel to obtain the total terminal current

$$I = 4100 \text{ A}$$

Thus the generated power, that is, the power fed to the voltage source at the terminals is

$$P = 615,000 \text{ W}.$$

The total pressure drop through the channel is

$$\Delta p = 2.11 \times 10^5 \text{ N/m}^2,$$
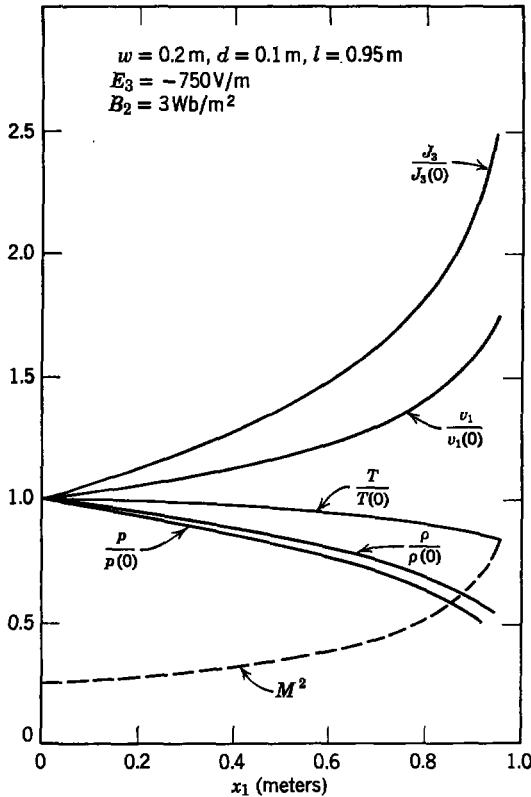
Fig. 13.2.3 Variation of properties along a constant-area channel with compressible flow acting as a generator.

or about 2.11 atm. It is interesting to compare these numbers with those of a generator that has an incompressible fluid operating with the same inlet velocity, electric field intensity, and flux density. Equations 12.2.19, 12.2.20, and 12.2.24 yield the results for the incompressible model:

$$I = 2850 \text{ A}, \qquad P = 427{,}000 \text{ W}, \qquad \Delta p = 0.95 \times 10^5 \text{ N/m}^2.$$

Comparison of these numbers with those of the compressible flow shows that with compressible flow the output current, power, and pressure drop are increased. Reference to the curves of Fig. 13.2.3 indicates that these increases are direct results of the increase in flow velocity with distance down the channel. The rather large difference in pressure drop is accounted for by the necessity to accelerate the gas flow in opposition to the decelerating $\mathbf{J} \times \mathbf{B}$ force.

This example has been presented to highlight some of the effects of compressibility. It must be emphasized that these results and the discussion hold only for *generator* operation with *subsonic* flow. For other conditions the effects can be grossly different. The techniques involved are the same, however.

13.2.2 Coupling with Steady Flow in a Variable-Area Channel

It is evident from the results of the preceding example that compressibility can limit the performance of a constant-area channel with MHD coupling; for example, with the conditions specified it would be impossible to operate the system with a larger pressure drop simply by lengthening the channel. Such limitations can be avoided by constructing the channel to make the cross-sectional area a function of distance (x_1) along the channel. When the channel area varies "slowly" enough with distance along the channel, we can use a *quasi-one-dimensional* model to describe the system with only one independent space variable. This technique is commonly employed in fluid mechanics* and magnetohydrodynamics,† and it yields quite accurate results in most applications. Its use in problems involving elastic media was introduced in Chapters 9 and 11. We present this technique in the context of a conduction-type MHD machine.

The system to be analyzed is illustrated in Fig. 13.2.4. It consists of a channel of rectangular cross-section but with the dimensions of the cross-section functions of the axial distance x_1. A perfect gas having constant electrical conductivity flows with velocity $\mathbf{v}$ through the channel as indicated
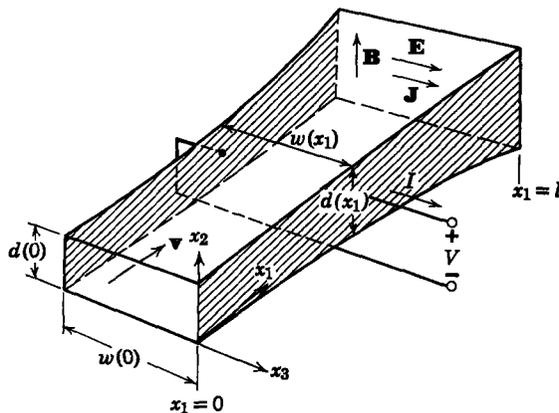
Fig. 13.2.4   MHD conduction machine with varying area.

* Shapiro, op. cit., pp. 73 and 74.
† Sutton and Sherman, op. cit., Chap. II.
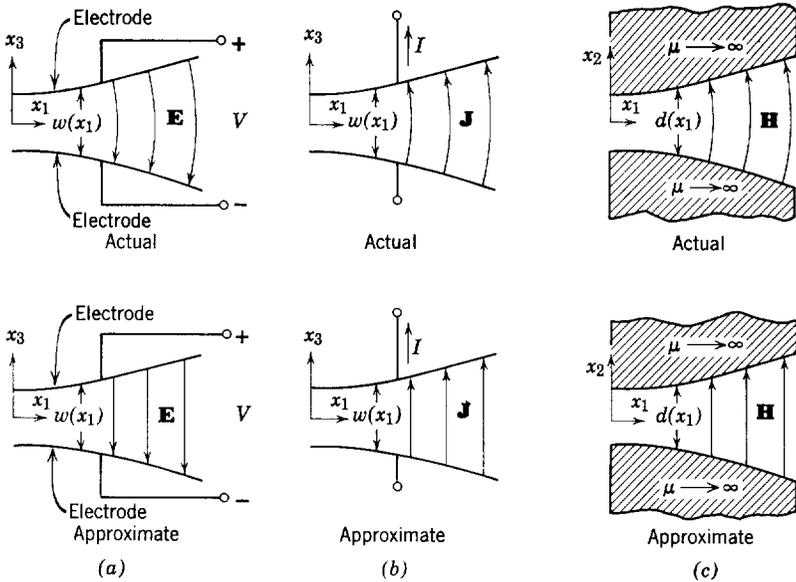
Fig. 13.2.5 Approximations for electromagnetic quantities in quasi-one-dimensional model: (*a*) electric field intensity; (*b*) current density; (*c*) magnetic field intensity.

in the figure. Two walls of the channel are insulators and two are electrodes that are connected to electrical terminals at which the terminal voltage V and terminal current I are defined with the polarities indicated.

We shall now develop the quasi-one-dimensional mathematical model for steady-flow in the system of Fig. 13.2.4. The derivation for non-steady flow is similar but more complex. The essential feature of the quasi-one-dimensional model is that all variables are assumed independent of x_2 and x_3 over a cross-section and they are thus functions only of x_1, the distance along the channel. This basic assumption involves approximations that will be discussed as we proceed.

We are considering a steady-flow problem; thus $(\partial/\partial t = 0)$ and the electric field is conservative $(\nabla \times \mathbf{E} = 0)$. The actual electric field lines between the electrodes will have the shapes shown qualitatively in Fig. 13.2.5*a*. In the quasi-one-dimensional model we assume that the field lines are only in the x_3-direction and the field intensity has the value

$$\mathbf{E} = \mathbf{i}_3 E_3 = -\mathbf{i}_3 \frac{V}{w(x_1)}. \tag{13.2.17}$$

This approximation is also illustrated in Fig. 13.2.5*a* and is the same as the long-wave limit used in the treatment of elastic continua in Chapters 9 and 10. It should be evident that the quality of the approximation improves as (dw/dx_1) becomes smaller.

The current density $\mathbf{J}$ will have the actual configuration shown in Fig. 13.2.5b. In the quasi-one-dimensional model we assume that $\mathbf{J}$ is in the x_3-direction:

$$\mathbf{J} = \mathbf{i}_3 J_3 \qquad (13.2.18)$$

and that J_3 is a function of x_1 only. This approximation is illustrated in Fig. 13.2.5b.

We neglect the magnetic field induced by current flow in the gas (low magnetic Reynolds number), thus within the gas $\nabla \times \mathbf{H} = 0$. For illustration purposes we assume infinitely permeable pole pieces that conform to the insulating walls of Fig. 13.2.4; consequently, the actual magnetic field intensity appears as in Fig. 13.2.5c. In the quasi-one-dimensional approximation the magnetic field intensity (and flux density because $\mathbf{B} = \mu_0\mathbf{H}$ in the gas) is in the x_2-direction and given by

$$\mathbf{H} = \mathbf{i}_2 \frac{F}{d(x_1)}, \qquad (13.2.19)$$

where F is the mmf (ampere-turns) applied by external means between the pole pieces. Thus

$$\mathbf{B} = \mathbf{i}_2 B_2(x_1) = \mathbf{i}_2 \frac{\mu_0 F}{d(x_1)}. \qquad (13.2.20)$$

This approximation, also illustrated in Fig. 13.2.5c, improves in validity as (dd/dx_1) decreases.

Although Fig. 13.2.5c represents a reasonable method for establishing the flux density, the magnetic material may not conform to the insulating walls or the field may be excited by air-core coils. In these cases we still assume that there is only an x_2-component of $\mathbf{B}$ and that it varies only with x_1 in a manner determined by the method of excitation. Thus $B_2(x_1)$ is most often a function independently set in the analysis of an MHD device.

It is clear from (13.2.17), (13.2.18), and (13.2.20) and Fig. 13.2.5 that fringing fields at the ends of the channel are neglected. It should also be clear that the approximate field quantities (13.2.17), (13.2.18) and (13.2.20) do not satisfy the required electromagnetic equations exactly. This is a consequence of the approximation.

In the quasi-one-dimensional model we assume that all the gas properties (p, ρ, T) are uniform over a cross section and functions only of x_1. Moreover, we assume that the x_1-component of the velocity is uniform over a cross section. We neglect the effects of transverse velocity components. Thus, in view of (13.2.17), (13.2.18) and (13.2.20), we write Ohm's law as

$$J_3 = \sigma(E_3 + v_1 B_2). \qquad (13.2.21)$$

Use of the small volume between planes at x_1 and at $x_1 + \Delta x_1$, as illustrated in Fig. 13.2.6 with the integral form of the conservation of mass (13.1.3) and the assumption of the uniformity of v_1 over a cross section gives

$$\oint (\rho \mathbf{v} \cdot \mathbf{n}) \, da = \rho(x_1 + \Delta x_1) v_1(x_1 + \Delta x_1) A(x_1 + \Delta x_1)$$

$$- \rho(x_1) v_1(x_1) A(x_1) = 0, \quad (13.2.22)$$

where A is the cross-sectional area given by

$$A(x_1) = w(x_1) \, d(x_1). \quad (13.2.23)$$

We divide (13.2.22) by Δx_1 and take the limit as $\Delta x_1 \to 0$ to obtain

$$\frac{d(\rho v_1 A)}{dx_1} = 0. \quad (13.2.24)$$

This is the differential form that expresses conservation of mass in the quasi-one-dimensional model.

In deriving the quasi-one-dimensional momentum equation it is often the practice to use a small volume, shown in Fig. 13.2.6, with the integral form of the momentum equation (13.1.5). It is more direct, however, to recognize initially the assumptions that all gas properties and the x_1-component of velocity are uniform over a cross section and that transverse components of velocity have negligible effects and to write the x_1-component of (13.1.4)

$$\rho v_1 \frac{dv_1}{dx_1} = - \frac{dp}{dx_1} - J_3 B_2. \quad (13.2.25)$$

In this equation we have used (13.1.9) for mechanical force density and $\mathbf{J} \times \mathbf{B}$ for the magnetic force density.

The same comments hold true for the conservation of energy. Recognizing the assumptions made, we can write the quasi-one-dimensional energy equation from (13.1.37) as

Fig. 13.2.6 Closed surface for derivation of conservation of mass equation for quasi-one-dimensional model.

$$\rho v_1 \frac{d}{dx_1} (h + \tfrac{1}{2} v_1^2) = J_3 E_3. \quad (13.2.26)$$

In the quasi-one-dimensional model the equations of state (13.1.10) and (13.1.14) or (13.1.36) are unchanged from their general forms.

The quasi-one-dimensional model of MHD interactions in the variable-area channel of Fig. 13.2.4 consists of (13.2.17), (13.2.18), (13.2.20), (13.2.21), (13.2.24), (13.2.25), (13.2.26), (13.1.10), and (13.1.36). This set of

coupled, nonlinear, differential equations can be used with specified boundary conditions to calculate how the gas properties, flow velocity, and electromagnetic quantities vary along the length of the channel. The equations are summarized in Table 13.2.1.

As is the case with compressible flow in a constant-area channel, (Section 13.2.1) it is useful to derive influence coefficients that express each derivative as a function of the variables themselves. These influence coefficients are useful for general interpretation of properties and for numerical integration of the equations.

By solving the equations in Table 13.2.1 for each of the derivatives separately we arrive at the following set of influence coefficients:

$$\frac{1}{v_1}\frac{dv_1}{dx_1} = \frac{1}{(1-M^2)}\left\{[(\gamma-1)E_3 + \gamma v_1 B_2]\frac{J_3}{\gamma p v_1} - \frac{1}{A}\frac{dA}{dx_1}\right\}, \qquad (13.2.27)$$

$$\frac{1}{\rho}\frac{d\rho}{dx_1} = \frac{1}{(1-M^2)}\left\{-[(\gamma-1)E_3 + \gamma v_1 B_2]\frac{J_3}{\gamma p v_1} + \frac{M^2}{A}\frac{dA}{dx_1}\right\}, \qquad (13.2.28)$$

$$\frac{1}{T}\frac{dT}{dx_1} = \frac{(\gamma-1)}{(1-M^2)}\left\{[(1-\gamma M^2)E_3 - \gamma M^2 v_1 B_2]\frac{J_3}{\gamma p v_1} + \frac{M^2}{A}\frac{dA}{dx_1}\right\}, \qquad (13.2.29)$$

$$\frac{1}{p}\frac{dp}{dx_1} = \frac{\gamma}{(1-M^2)}\left\{-[(\gamma-1)M^2 E_3 + \{1 + (\gamma-1)M^2\}v_1 B_2]\right.$$
$$\left. \times \frac{J_3}{\gamma p v_1} + \frac{M^2}{A}\frac{dA}{dx_1}\right\}, \qquad (13.2.30)$$

$$\frac{1}{M^2}\frac{dM^2}{dx_1} = \frac{\gamma}{(1-M^2)}\left\{[(\gamma-1)(1+\gamma M^2)E_3 + \gamma\{2 - (\gamma-1)M^2\}v_1 B_2]\frac{J_3}{\gamma p v_1}\right.$$
$$\left. - \frac{[2 + (\gamma-1)M^2]}{A}\frac{dA}{dx_1}\right\}. \qquad (13.2.31)$$

These influence coefficients should be compared with those of (13.2.13) to (13.2.16) for the constant-area channel. It is clear that when $(dA/dx_1 = 0)$ the two sets of influence coefficients become identical.

It is also clear from (13.2.27) to (13.2.31) that for any set of conditions the derivative of any variable can be made to have either sign and any magnitude by adjusting the factor (dA/dx_1). Thus the tendency of the flow to approach Mach one in a constant-area channel can be counteracted by letting the area of the channel vary. In fact, by adjusting the area $A(x_1)$ such that the quantity in braces in (13.2.31) is zero all along the channel the Mach number can be held constant along the channel. It is also true that any of the other influence coefficients can be used to design a channel [fix $A(x_1)$] such that one property $(v_1, \rho, p, \text{ or } T)$ is constant along the length of the channel.

Table 13.2.1   Summary of Quasi-One-Dimensional Equations for System
of Fig. 13.2.4

Channel area	$A(x_1) = w(x_1)\,d(x_1)$	(13.2.23)
Electric field intensity	$\mathbf{E} = \mathbf{i}_3 E_3 = -\mathbf{i}_3 \dfrac{V}{w(x_1)}$	(13.2.17)
Current density	$\mathbf{J} = \mathbf{i}_3 J_3$	(13.2.18)
Magnetic flux density	$\mathbf{B} = \mathbf{i}_2 B_2(x_1)$	(13.2.20)
Ohm's law	$J_3 = \sigma(E_3 + v_1 B_2)$	(13.2.21)
Conservation of mass	$\dfrac{d(\rho v_1 A)}{dx_1} = 0$	(13.2.24)
Conservation of momentum	$\rho v_1 \dfrac{dv_1}{dx_1} = -\dfrac{dp}{dx_1} - J_3 B_2$	(13.2.25)
Conservation of energy	$\rho v_1 \dfrac{d}{dx_1}(h + \tfrac{1}{2}v_1^2) = J_3 E_3$	(13.2.26)
Mechanical equation of state	$p = \rho R T$	(13.1.10)
Thermal equation of state	$dh = c_p\,dT$	(13.1.36)
Local sound velocity	$a = \sqrt{\gamma R T}$	(13.2.11)
Local Mach number	$M = \dfrac{v_1}{a}$	(13.2.12)

Although the influence coefficients of (13.2.27) to (13.2.31) are useful for examining general properties of the variable-area MHD machine and for numerical integration when necessary, some exact solutions are possible and they are best obtained by using the basic equations summarized in Table 13.2.1.

Before proceeding with an example of an exact solution of the equations it is useful to introduce a convention used in the analysis of gaseous MHD generators. This convention defines a loading factor K as

$$K = -\frac{E_3}{v_1 B_2}. \tag{13.2.32}$$

The use of the factor K in Ohm's law (13.2.21) yields

$$J_3 = (1 - K)\sigma v_1 B_2. \tag{13.2.33}$$

Thus, when $0 < K < 1$, electric energy is being extracted from the gas; otherwise it is being put into the gas. The power density extracted electrically *from* the gas [see (13.2.26)] is

$$p_e = -J_3 E_3 = K(1 - K)\sigma v_1^2 B_2^2. \tag{13.2.34}$$

Thus it is evident that maximum energy is extracted locally when $K = \frac{1}{2}$ or when the electric field intensity is one half $\mathbf{v} \times \mathbf{B}$. On a continuum basis this is the maximum output condition when the external impedance is made equal to internal impedance. In general, K can be a function of x_1; however, to achieve maximum power extraction along the channel, K should be kept close to the optimum value of one half. It is evident from (13.2.34) that the maximum power density that can be extracted electrically from the gas is

$$p_{e(\text{max})} = \frac{\sigma v_1^2 B_2^2}{4}. \tag{13.2.35}$$

We now set constraints suitable for obtaining an exact solution of the quasi-one-dimensional equations that describe the variable area MHD machine in Fig. 13.2.4. A set of constraints is selected to correspond closely to those used for analyzing MHD generators for large amounts of power (more than 100 MW). We present a normalized solution in literal form and then introduce numerical constants.

It is assumed that the values of all quantities are known at the inlet ($x_1 = 0$). We select the channel dimensions to achieve constant flow velocity v_1, constant loading factor K, and constant-channel aspect ratio $[w(x_1)/d(x_1)]$. The requirements of constant K and constant aspect ratio are satisfied only if

$$B_2 \sim \frac{1}{d(x_1)}.$$

Thus we assume that the magnetic field is excited by using infinitely permeable pole pieces that conform to the insulating walls, as illustrated in Fig. 13.2.5c. It follows that the flux density B_2 is given by (13.2.20).

For the constraints that have been specified, with the loading factor K defined by (13.2.32) and the current density J_3 given by (13.2.33), the equations of Table 13.2.1 can be simplified to the following:

$$\frac{d(\rho A)}{dx_1} = 0, \tag{13.2.36}$$

$$\frac{dp}{dx_1} = -(1 - K)\sigma v_1 B_2^2, \tag{13.2.37}$$

$$\rho v_1 c_p \frac{dT}{dx_1} = -K(1 - K)\sigma v_1^2 B_2^2, \tag{13.2.38}$$

$$p = \rho R T. \tag{13.2.39}$$

Before solving for any variable as a function of x_1, it is convenient to obtain relations between pairs of unknowns; for example, division of (13.2.38) by

(13.2.37) and simplification of the results yield

$$\rho c_p \frac{dT}{dx_1} = K \frac{dp}{dx_1}.$$ (13.2.40)

This equation can be written as

$$(\rho R T)\left(\frac{c_p}{R}\right)\frac{1}{T}\frac{dT}{dx_1} = (Kp)\frac{1}{p}\frac{dp}{dx_1}.$$ (13.2.41)

Using (13.2.39) and the fact that

$$\frac{c_p}{R} = \frac{\gamma}{\gamma - 1},$$

we integrate (13.2.41) to obtain the result that

$$\frac{p(x_1)}{p(0)} = \left[\frac{T(x_1)}{T(0)}\right]^{\gamma/[K(\gamma-1)]}$$ (13.2.42)

Note from (13.2.33) that when $K = 1$ no current flows and (13.2.42) reduces to the standard isentropic relation between temperature and pressure.*
    We now use (13.2.42) with (13.2.39) to obtain the relation between temperature and density as

$$\frac{\rho(x_1)}{\rho(0)} = \left[\frac{T(x_1)}{T(0)}\right]^{[\gamma-K(\gamma-1)]/K(\gamma-1)}$$ (13.2.43)

The use of this result with (13.2.36) yields

$$\frac{A(x_1)}{A(0)} = \left[\frac{T(x_1)}{T(0)}\right]^{[K(\gamma-1)-\gamma]/K(\gamma-1)}$$ (13.2.44)

Because the aspect ratio (w/d) is constant, (13.2.44) yields the result

$$\frac{d(x_1)}{d(0)} = \frac{w(x_1)}{w(0)} = \left[\frac{A(x_1)}{A(0)}\right]^{1/2}$$ (13.2.45)

Finally, the definition of Mach number M in Table 13.2.1 with the constraint of constant velocity yields the relation between the square of the Mach number and the temperature:

$$\frac{M^2(x_1)}{M^2(0)} = \left[\frac{T(x_1)}{T(0)}\right]^{-1}.$$ (13.2.46)

    Now that we have relations among the unknowns it is necessary to obtain a solution for only one of the unknowns as a function of x_1. It is easiest to

* Allis and Herlin, op. cit., p.78.

do this for the temperature by using (13.2.38), which we rewrite as

$$\frac{dT}{dx_1} = \frac{-K(1 - K)\sigma v_1 B_2{}^2}{\rho c_p},$$ (13.2.47)

From (13.2.36) $\rho A = $ constant and from (13.2.20) and (13.2.45) $B_2{}^2 A = $ constant.

Thus (13.2.47) becomes

$$\frac{dT}{dx_1} = - \frac{K(1 - K)\sigma v_1 B_2{}^2(0)}{\rho(0)c_p}.$$ (13.2.48)

The right side of this expression is constant and integration yields

$$T(x_1) - T(0) = - \frac{K(1 - K)\sigma v_1 B_2{}^2(0)}{\rho(0)c_p} x_1.$$ (13.2.49)

By normalizing and rearranging this expression we obtain

$$\frac{T(x_1)}{T(0)} = 1 - \frac{(\gamma - 1)\, K(1 - K)\sigma v_1\, B_2{}^2(0)}{\gamma p(0)} x_1.$$ (13.2.50)

We define the constant C_1 as

$$C_1 = \frac{(\gamma - 1)\, K(1 - K)\sigma v_1\, B_2{}^2(0)}{\gamma p(0)}.$$ (13.2.51)

and rewrite (13.2.50) as

$$\frac{T(x_1)}{T(0)} = 1 - C_1 x_1.$$ (13.2.52)

We now use (13.2.42) to (13.2.46) to obtain the space variations of the other variables; thus

$$\frac{p(x_1)}{p(0)} = (1 - C_1 x_1)^{\gamma/[K(\gamma-1)]},$$ (13.2.53)

$$\frac{\rho(x_1)}{\rho(0)} = (1 - C_1 x_1)^{[\gamma - K(\gamma-1)]/K(\gamma-1)},$$ (13.2.54)

$$\frac{A(x_1)}{A(0)} = (1 - C_1 x_1)^{[K(\gamma-1)-\gamma]/K(\gamma-1)},$$ (13.2.55)

$$\frac{d(x_1)}{d(0)} = \frac{w(x_1)}{w(0)} = (1 - C_1 x_1)^{[K(\gamma-1)-\gamma]/2K(\gamma-1)},$$ (13.2.56)

$$\frac{M^2(x_1)}{M^2(0)} = (1 - C_1 x_1)^{-1}.$$ (13.2.57)

To complete the description of this generator we note from (13.2.17) and (13.2.32) that the terminal voltage with polarity defined in Fig. 13.2.4 is

$$V = K v_1 B_2(x_1)\, w(x_1) \tag{13.2.58}$$

and constant. From (13.2.33) the current density is

$$J_3 = (1 - K)\sigma v_1\, B_2(x_1). \tag{13.2.59}$$

The total terminal current is

$$I = \int_0^l J_3\, d(x_1)\, dx_1 = \int_0^l (1 - K)\sigma v_1\, B_2(x_1)\, d(x_1)\, dx_1. \tag{13.2.60}$$

From (13.2.20) we have

$$B_2(x_1)\, d(x_1) = B_2(0)\, d(0); \tag{13.2.61}$$

thus (13.2.60) is written as

$$I = \int_0^l (1 - K)\sigma v_1\, B_2(0)\, d(0)\, dx_1. \tag{13.2.62}$$

In this expression the integrand is constant, which indicates that each element dx_1 along the length makes the same contribution to the total current. Integration of (13.2.62) yields

$$I = (1 - K)\sigma v_1\, B_2(0)\, d(0)l. \tag{13.2.63}$$

It is interesting to note by reference to Section 12.2.1 that this is the same as the current output from a constant-area channel of depth $d(0)$, width $w(0)$, and length l, using an incompressible fluid with conductivity σ and velocity v_1 in the presence of a uniform flux density of value $B_2(0)$.

It will be instructive to make the input dimensions and variables the same as those of the constant-area channel in Section 13.2.1 and to compare the performance of the variable area and constant-area channels. Thus we set

$R = 250$ J/kg°K,	$\gamma = 1.4$,	$c_p = 875$ J/kg°K,
$\sigma = 40$ mhos/m,	$v_1 = 500$ m/sec,	$T(0) = 3000$°K,
$p(0) = 4 \times 10^5$ N/m²,	$\rho(0) = 0.534$ kg/m³,	$M^2(0) = 0.238$,
$w(0) = 0.2$ m,	$d(0) = 0.1$ m,	$l = 0.95$ m,
$K = \frac{1}{2}$,	$V = 150$ V,	$B_2(0) = 3$ Wb/m².

First we use (13.2.51) to calculate the constant C_1:

$$C_1 = 0.0322/\text{m}.$$

Then the expressions for the variables follow from (13.2.52) to (13.2.57):

$$\frac{T(x_1)}{T(0)} = (1 - 0.0322x_1), \qquad\qquad \frac{p(x_1)}{p(0)} = (1 - 0.0322x_1)^7,$$

$$\frac{\rho(x_1)}{\rho(0)} = (1 - 0.0322x_1)^6, \qquad\qquad \frac{A(x_1)}{A(0)} = \frac{1}{(1 - 0.0322x_1)^6},$$

$$\frac{d(x_1)}{d(0)} = \frac{w(x_1)}{w(0)} = \frac{1}{(1 - 0.0322x_1)^3}, \qquad M^2(x_1) = \frac{0.238}{(1 - 0.0322x_1)}.$$

These variations with x_1 are plotted in Fig. 13.2.7. Compare the curves in this figure with those in Fig. 13.2.3 to learn how the slight variation of the channel area can reduce the changes in properties along the channel. Because the Mach number has changed so slightly over the length of the channel, the channel can be made much longer without reaching Mach one. This was not the case for the constant-area channel.

Further comparisons can be made in the constant-area channel with both compressible and incompressible fluids. Assuming the same inlet dimensions and properties for each of the three cases, we list several quantities in Table 13.2.2. Note that the constant-area generator with incompressible fluid produces the same power as the variable-area generator but with a larger pressure drop, and that the constant-area generator with compressible fluid produces the most power. This is due to the acceleration of the gas down the channel, as indicated by Fig. 13.2.3. This small increase in power occurs at the expense of a large increase in pressure and temperature drops
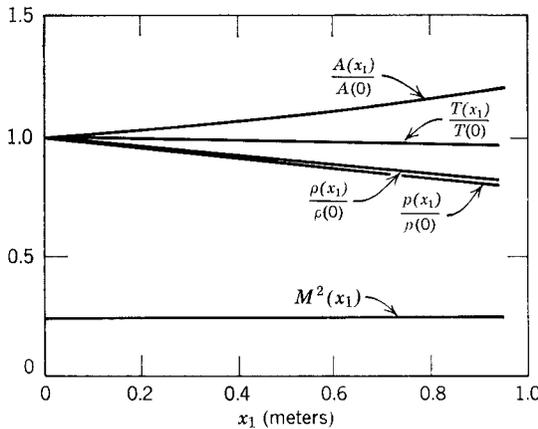
Fig. 13.2.7 Variation of properties along a variable-area channel designed to have constant velocity and constant loading factor while acting as a generator.

Table 13.2.2 Properties of MHD Generators

	Constant-Area Incompressible Fluid	Constant-Area Compressible Fluid	Variable-Area Constant Velocity Constant Loading Factor
Terminal voltage (volts)	150	150	150
Terminal current (amperes)	2,850	4,100	2,850
Power output (watts)	427,000	615,000	427,000
Pressure drop (newtons per square meter)	0.95×10^5	2.11×10^5	0.80×10^5
Temperature drop (degrees Kelvin)	...	420	93

over the variable-area generator. Although it is beyond the scope of this book, it is worthwhile to remark that this increase in power output from the constant-area channel results in the generation of considerable entropy which makes the energy in the exhaust fluid less available than with the variable-area channel.

In our analysis of the variable area channel we defined a set of constraints that allowed the complete solution of the differential equations in closed form. Several other sets of constraints allow direct integration of the equations. For still others numerical integration is necessary for solution.

It must be recognized that when a set of constraints is selected and closed-form solutions are obtained the design of a generator is fixed. In our example this means we specify the dimensions $[d(x_1)$, and $w(x_1)]$. Now, if we wish to operate this channel with a different set of inlet conditions, magnetic flux density, and/or applied voltage, we can no longer, in general, determine how the properties vary along the channel by literal integration. Instead, we must integrate numerically. Thus, if we wanted to fix the inlet properties to the channel we designed in our example and to find the output current and power as a function of load resistance for the range from open-circuit to short circuit, our solution in closed form would represent only one point on the curve. The remainder of the points would have to be found by numerical integration.

The preceding analysis of a variable-area MHD machine with a compressible working fluid is the basic technique in the study of electromechanical coupling in conduction-type MHD generators. Several types of machine have been built or proposed.* A cutaway drawing of one machine is shown in Fig. 13.2.8 and a photograph in Fig. 13.2.9.

* T. R. Brogan, "MHD Power Generation," *IEEE Spectrum*, 1, 58–65 (February 1964).

Power output
leads

Channel power
output section

Channel self
excitation section

Exhaust pipe

Copper magnet
windings

Combustion
chamber

Magnet structural
reinforcements
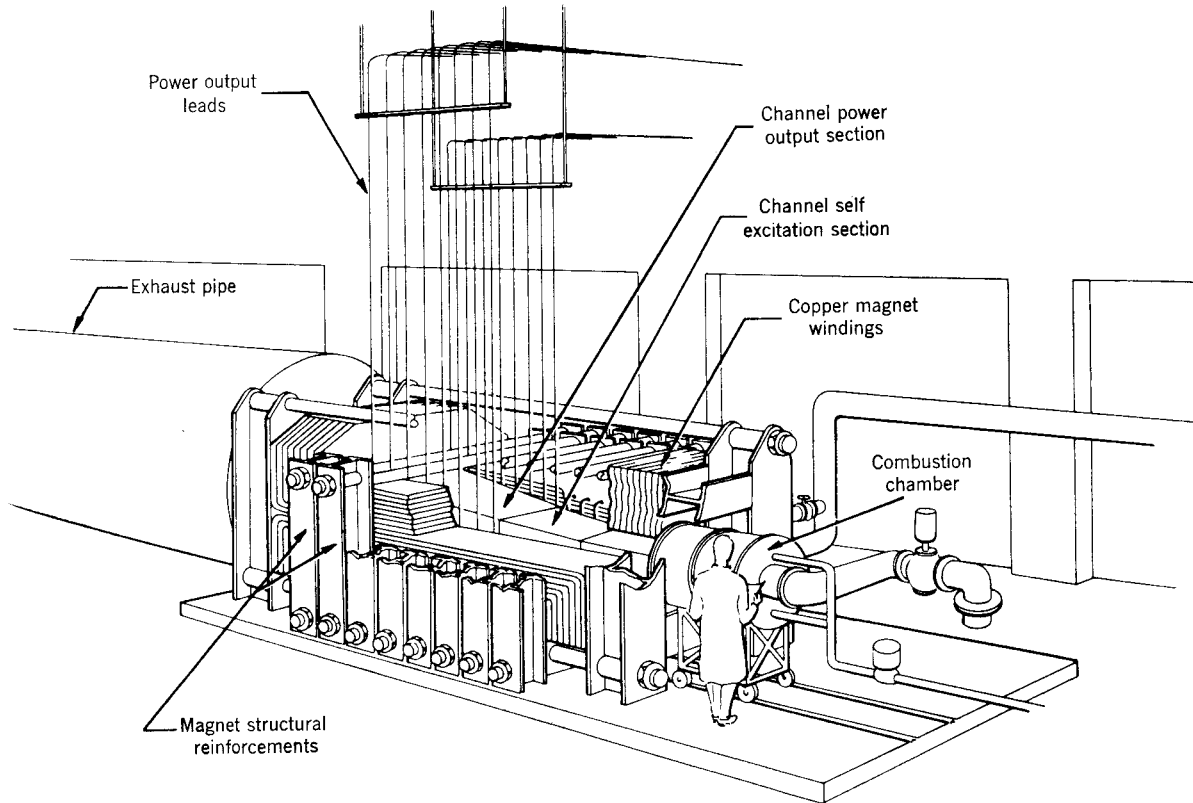
Fig. 13.2.8 Cutaway drawing of Avco Mark V rocket-driven, self-excited MHD power generator. Oxygen and fuel are burned in the combustion chamber to create a 5000°F electrically conducting gas which flows through the channel, where it interacts with the magnetic field to generate power. The magnet coil is excited by part of the generator output. For a gross power output of 31.3 MW, 7.7 MW are used to energize the field coils. (Courtesy of Avco-Everett Research Laboratory, a division of Avco Corporation.)

Courtesy of Textron Corporation. Used with permission.
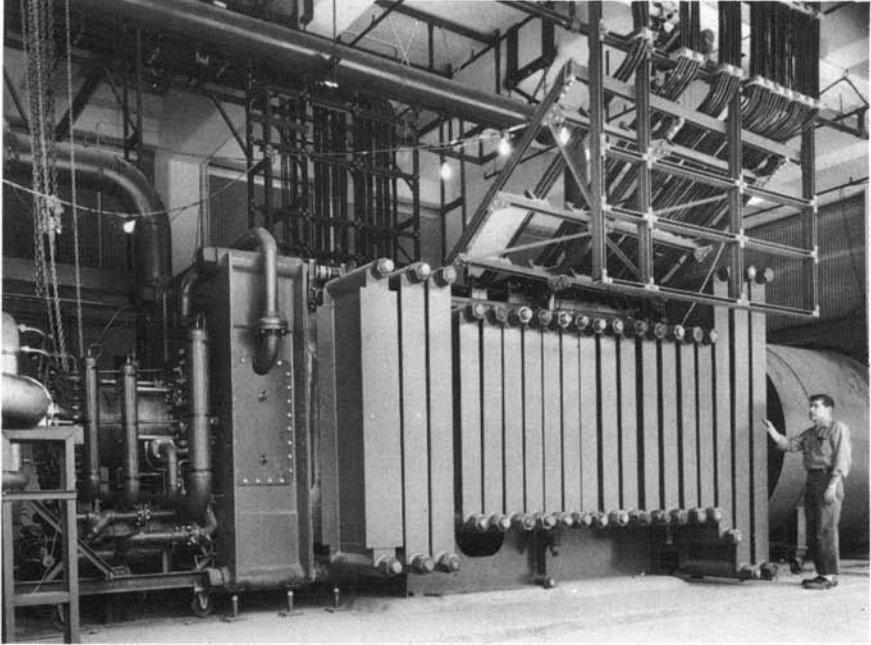
Fig. 13.2.9 Photograph of Avco Mark V generator described in Fig. 13.2.8. (Courtesy of Avco-Everett Research Laboratory, a division of Avco Corporation.)

Courtesy of Textron Corporation. Used with permission.

13.2.3 Coupling with Propagating Disturbances

Recall from Section 12.2.3 that in the analysis of Alfvén waves propagating through an incompressible fluid of high electrical conductivity the fluid motion was entirely transverse. Even though the assumption of incompressibility was made, it was not necessary for the type of fluid motion described. Thus Alfvén waves are also found in an inviscid gas of high electrical conductivity.

Because a gas is compressible, it will also transmit longitudinal (acoustic) waves that are very much like the longitudinal elastic waves analyzed in Chapter 11. The propagation of acoustic waves in a gas can be affected by bulk electromechanical coupling when the gas has high electrical conductivity and is immersed in a transverse magnetic field. These modified disturbances are called magnetoacoustic waves. The same phenomena also occur in liquids because liquids are slightly compressible. The effect of bulk electromechanical coupling on acoustic waves in a liquid, however, is much less pronounced than in a gas. Consequently, we use our mathematical model of a gas to describe acoustic waves first and then to describe magnetoacoustic waves.

13.2.3a   Acoustic Waves

As already stated, we shall study longitudinal disturbances, and thus we assume the rectangular channel in Fig. 13.2.10, which has rigid walls perpendicular to the x_2- and x_3-axes and infinite length in the x_1-direction. At $x_1 = 0$ a close-fitting piston, perpendicular to the x_1-direction, can be driven in the x_1-direction by a mechanical source. The channel is filled with a gas, with gas constant R and specific heat capacity at constant volume c_v, that can be represented as ideal. With this arrangement, the piston will drive disturbances that are uniform across the channel and that will propagate along the channel. The infinite length in the x_1-direction precludes reflections of the disturbance.

It is clear from the configuration of Fig. 13.2.10 that with disturbances driven by the piston uniformly in an x_2-x_3-plane there will be no variation of properties with x_2 or x_3 and there will only be an x_1-component of velocity v_1. Thus we can write the equations of motion for the gas in one-space-dimensional forms:

conservation of mass (13.1.1)

$$\frac{D_1 \rho}{Dt} = -\rho \frac{\partial v_1}{\partial x_1}, \tag{13.2.64}$$

where now

$$\frac{D_1}{Dt} = \left(\frac{\partial}{\partial t} + v_1 \frac{\partial}{\partial x_1} \right), \tag{13.2.65}$$

conservation of momentum (13.1.17)

$$\rho \frac{D_1 v_1}{Dt} = \frac{\partial p}{\partial x_1}, \tag{13.2.66}$$

conservation of energy (13.1.29)

$$\rho \frac{D_1}{Dt} (u + \tfrac{1}{2} v_1^2) = - \frac{\partial}{\partial x_1} (pv_1), \tag{13.2.67}$$

and the equations of state (13.1.10) and (13.1.14)

$$p = \rho R T, \qquad du = c_v \, dT. \tag{13.2.68}$$

Before proceeding to analyze the propagation of disturbances, it will be useful to simplify the equations somewhat. First, we use the equations of state to eliminate u and then T from the conservation of energy.

$$\rho \frac{c_v}{R} \frac{D_1}{Dt} \left(\frac{p}{\rho} \right) + \rho v_1 \frac{D_1 v_1}{Dt} = - \frac{\partial}{\partial x_1} (pv_1). \tag{13.2.69}$$
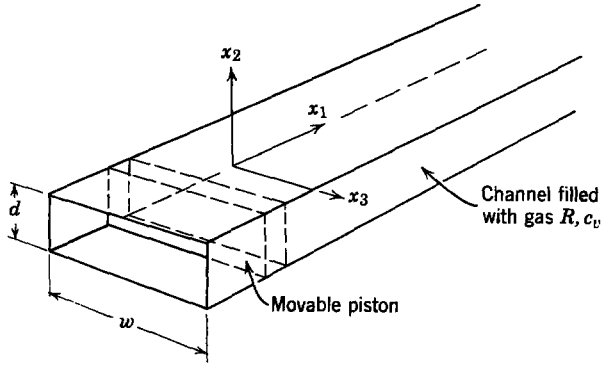
Fig. 13.2.10 Configuration for studying propagation of longitudinal (acoustic) disturbances in a gas.

Next, the conservation of momentum equation simplifies this expression to

$$\rho \frac{c_v}{R} \frac{D_1}{Dt}\left(\frac{p}{\rho}\right) = -p \frac{\partial v_1}{\partial x_1}. \tag{13.2.70}$$

Finally, the conservation of mass equation eliminates the space derivative of v_1 and the derivative on the left is expanded to obtain

$$\frac{D_1 p}{Dt} = \frac{\gamma p}{\rho} \frac{D_1 \rho}{Dt}. \tag{13.2.71}$$

An equation of the same form can be obtained for three-dimensional variations of properties.

Equations 13.2.64, 13.2.66, and 13.2.71 are sufficient to describe the propagation of disturbances through the gas; these equations, however, are nonlinear. For the remainder of this section, we assume that the disturbances involve small perturbations from an equilibrium condition such that the equations can be linearized. Thus we represent the three relevant variables in terms of equilibrium quantities (subscript o) and perturbation quantities (primed)

$$p = p_o + p', \tag{13.2.72a}$$

$$\rho = \rho_o + \rho', \tag{13.2.72b}$$

$$v_1 = v_1'. \tag{13.2.72c}$$

At equilibrium the gas is at rest; thus the equilibrium value of v_1 is zero.

Substitution of (13.2.72a–c) into (13.2.64), (13.2.66), and (13.2.71) and

retention of only linear terms in the perturbation quantities yield

$$\frac{\partial \rho'}{\partial t} = -\rho_o \frac{\partial v_1'}{\partial x_1},$$

(13.2.73)

$$\rho_o \frac{\partial v_1'}{\partial t} = -\frac{\partial p'}{\partial x_1},$$

(13.2.74)

$$p' = \frac{\gamma p_o}{\rho_o} \rho'.$$

(13.2.75)

In obtaining (13.2.75), the linearized version of (13.2.71) has been integrated and the constant of integration set to zero because both perturbation quantities are zero at equilibrium.

Elimination of p' and ρ' from (13.2.73) to (13.2.75) yields a single equation with v_1' as the unknown:

$$\frac{\partial^2 v_1'}{\partial t^2} = \frac{\gamma p_o}{\rho_o} \frac{\partial^2 v_1'}{\partial x_1^2}.$$

(13.2.76)

This is a wave equation (see Section 11.4.1) that describes longitudinal (acoustic) waves that propagate with a sound speed given by*

$$a_s = \left(\frac{\gamma p_o}{\rho_o}\right)^{1/2}.$$

(13.2.77)

Refer now to Fig. 13.2.10. We specify that the piston be driven with small amplitude oscillations such that the velocity of the gas at $x_1 = 0$ is constrained to be

$$v_1'(0, t) = V_m \cos \omega t.$$

(13.2.78)

Because the channel is infinitely long in the x_1-direction, disturbances will propagate only in the positive x_1-direction (there are no reflected waves). Thus the velocity of the gas at any point along the channel for steady-state conditions is

$$v_1'(x_1, t) = V_m \cos\left(\omega t - \frac{\omega}{a_s} x_1\right).$$

(13.2.79)

That this is a solution of (13.2.76) which satisfies the boundary condition of (13.2.78) can be verified by direct substitution.

We can now use (13.2.79) in (13.2.73) to find the perturbation density

$$\rho'(x_1, t) = \rho_o \frac{V_m}{a_s} \cos\left(\omega t - \frac{\omega}{a_s} x_1\right).$$

(13.2.80)

* This is the same speed as that given by (13.2.11).
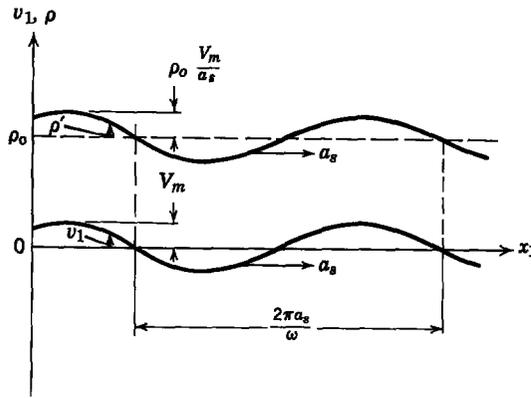
Fig. 13.2.11   Density and velocity variations in a sound wave of frequency ω propagating in the positive x_1-direction.

Sketches of the variation of density and velocity as functions of space at a given instant of time are shown in Fig. 13.2.11. Note that the velocity and density perturbations are in phase and that the whole pattern propagates in the positive x_1-direction with the acoustic speed a_s.

It is clear from the nature of the wave equation (13.2.76) that sound waves propagate in our assumed perfect medium without dispersion. Thus all the techniques and conclusions of Section 9.1.1 apply equally well to sound waves.

It is also worthwhile at this point to comment that no heat conduction term appears in the conservation of energy equation. This is the model that best describes sound waves from the audio-frequency range up to the megacycle per second range.

In modeling the slight compressibility of liquids to describe mechanical behavior during moderate changes in pressure the temperature is immaterial. Consequently, the conservation of energy equation and the thermal equation of state are dropped, and the mechanical equation of state is conventionally written as*

$$\frac{d\rho}{\rho} = \kappa \, dp, \qquad (13.2.81)$$

where κ is the compressibility. For small perturbations about an equilibrium with the definitions of (13.2.72a,b) (13.2.81) can be linearized and integrated to obtain

$$p' = \frac{1}{\kappa \rho_o} \rho'. \qquad (13.2.82)$$

* See, for example, H. B. Callen, *Thermodynamics*, Wiley, New York, 1960, pp. 344–349.

If this expression is used in place of (13.2.75) with (13.2.73) and (13.2.74), it will be found that a wave equation like that of (13.2.76) will result and $(\gamma p_o/\rho_o)$ will be replaced by $(1/\kappa\rho_o)$. Thus for a liquid with density ρ_o and compressibility κ the acoustic speed is

$$a_s = \frac{1}{\sqrt{\kappa\rho_o}}. \tag{13.2.83}$$

With this modification all the results already obtained for acoustic waves in inviscid gases hold equally well for acoustic waves in inviscid liquids.

In this mathematical development we used a lossless fluid model with the mathematical result that a plane disturbance propagates with no attenuation. In all real fluids viscosity (mechanical loss) dissipates energy and damps disturbances. In most practical problems, however, the damping is slight and can be treated mathematically as a perturbation of the lossless analysis, much like the process used to introduce electrical losses in transmission lines.† Although the problem of viscous damping of acoustic waves is not analyzed in this book, the concept and mathematical model of viscosity is introduced in Chapter 14, and it is a straightforward process to include viscous terms as perturbations on the lossless analysis and evaluate viscous damping of acoustic waves.

13.2.3b Magnetoacoustic Waves

Now that we have described the physical nature and mathematical characterization of ordinary acoustic waves, we add bulk electromechanical coupling to see how acoustic waves are modified to magnetoacoustic waves. The physical system to be used is the rectangular channel of Fig. 13.2.10, with electric and magnetic modifications, as illustrated in Fig. 13.2.12. The channel is fitted with pole pieces and an excitation winding which produce, at equilibrium, a flux density that is uniform throughout the channel and has only an x_2-component:

$$\mathbf{B} = \mathbf{i}_2 B_o. \tag{13.2.84}$$

The walls of the channel that are perpendicular to the x_3-axis are made of highly conducting electrodes. The movable piston is also made of highly conducting material.

Because of the high conductivity of the gas, the electrodes, and the piston and because of the presence of an applied magnetic field, the electromagnetic part of this system is represented by a quasi-static, magnetic field system.

† See, for example, R. B. Adler, L. J. Chu, and R. M. Fano, *Electromagnetic Energy Transmission and Radiation*, Wiley, New York, 1960, Chapter 5, p. 179.
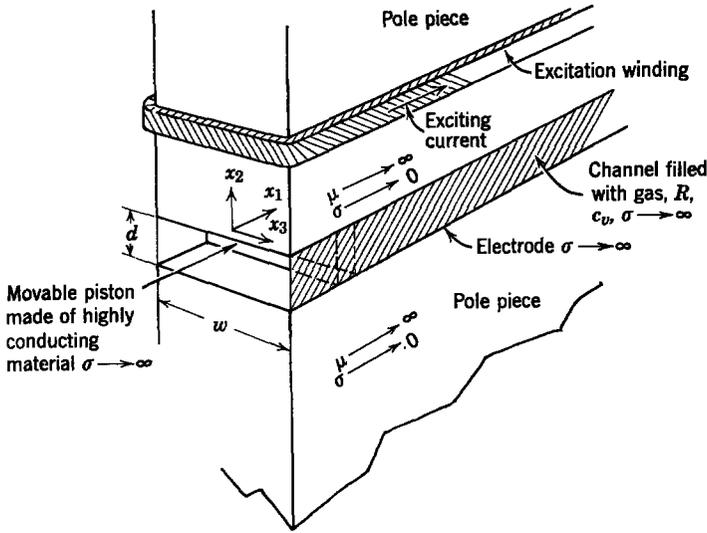
Fig. 13.2.12 Configuration for studying propagation of magnetoacoustic disturbances in a highly conducting gas.

Moreover, the assumed symmetry in the problem (including a neglect of fringing effects at the ends and edges of the channel) leads to the conclusion that, as in the preceding section, all variables are independent of x_2 and x_3. Furthermore, the gas velocity has only an x_1-component v_1, the highly conducting electrodes cause the electric field intensity to have only an x_3-component E_3, the current density in the gas thus also has only an x_3-component,* and the perturbation magnetic field induced by current flow in the gas has only an x_2-component. Summarizing these statements about electromagnetic quantities, we have

$$\mathbf{E} = \mathbf{i}_3 E_3(x_1, t), \tag{13.2.85a}$$

$$\mathbf{J} = \mathbf{i}_3 J_3(x_1, t), \tag{13.2.85b}$$

$$\mathbf{B} = \mathbf{i}_2[B_o + B_2'(x_1, t)]. \tag{13.2.85c}$$

In order to describe mathematically the dynamic nature of magnetoacoustic waves, we must modify (13.2.64) to (13.2.68) to include electromechanical coupling terms and add the electromagnetic equations necessary for a complete description.

---

* As we shall see subsequently, there is longitudinal current in the electrodes to satisfy $\nabla \cdot \mathbf{J} = 0$.

First, the momentum and energy equations (13.2.66) and (13.2.67) must be modified to include coupling terms, thus:

conservation of momentum (13.1.17) is

$$\rho \frac{D_1 v_1}{Dt} = - \frac{\partial p}{\partial x_1} - J_3(B_o + B_2'), \qquad (13.2.86)$$

and conservation of energy (13.1.29) is

$$\rho \frac{D_1}{Dt}(u + \tfrac{1}{2}v_1^2) = - \frac{\partial}{\partial x_1}(pv_1) + J_3 E_3. \qquad (13.2.87)$$

Next, recognizing that the equilibrium flux density B_o is not a function of time or space, the relevant electromagnetic equations are:

Ampere's law (1.1.1)*

$$\frac{1}{\mu_0} \frac{\partial B_2'}{\partial x_1} = J_3, \qquad (13.2.88)$$

Faraday's law (1.1.5)*

$$\frac{\partial E_3}{\partial x_1} = \frac{\partial B_2'}{\partial t}, \qquad (13.2.89)$$

and Ohm's law $\mathbf{J'} = \sigma \mathbf{E'}$ written as†

$$J_3 = \sigma[E_3 + v_1(B_o + B_2')]. \qquad (13.2.90)$$

Note that $\nabla \cdot \mathbf{B} = 0$ is automatically satisfied by the functional form of $\mathbf{B}$ that results in this problem.

The equations necessary for describing magnetoacoustic disturbances are (13.2.86) to (13.2.90), plus the conservation of mass (13.2.64) and the equations of state (13.2.68). As in the case of acoustic waves, these equations are nonlinear; thus we assume perturbations small enough to allow us to linearize the equations of motion. Again we represent the relevant variables in terms of equilibrium quantities (subscript o) and perturbation quantities (primed).

$$p = p_o + p', \qquad (13.2.91a)$$
$$\rho = \rho_o + \rho', \qquad (13.2.91b)$$
$$T = T_o + T', \qquad (13.2.91c)$$
$$v_1 = v_1', \qquad (13.2.91d)$$
$$B_2 = B_o + B_2', \qquad (13.2.91e)$$
$$J_3 = J_3', \qquad (13.2.91f)$$
$$E_3 = E_3'. \qquad (13.2.91g)$$

* Table 1.2, Appendix G.
† See Table 6.1, Appendix G.

Note that velocity, current density, and electric field intensity have zero equilibrium values.

First, linearization of Ohm's law (13.2.90) in the limit where $\sigma \to \infty$ gives

$$E_3 = -v_1 B_o. \tag{13.2.92}$$

Substitution of this result in (13.2.89) yields

$$\frac{1}{B_o} \frac{\partial B_2'}{\partial t} = -\frac{\partial v_1'}{\partial x_1}. \tag{13.2.93}$$

Linearization of (13.2.64) (conservation of mass) and division of the result by ρ_o yields

$$\frac{1}{\rho_o} \frac{\partial \rho'}{\partial t} = -\frac{\partial v_1'}{\partial x_1}. \tag{13.2.94}$$

Subtraction of (13.2.94) from (13.2.93) and integration with respect to time (recognizing that for equilibrium conditions all perturbation quantities go to zero) yields

$$\frac{B_2'}{B_o} = \frac{\rho'}{\rho_o}. \tag{13.2.95}$$

This shows that perturbations in flux density follow perturbations in mass density. This is formal mathematical acknowledgment that for $\sigma \to \infty$ the time constant for diffusion of magnetic flux lines through the gas goes to infinity and the flux lines are essentially frozen into the material.

It can be verified by following a process similar to that for (13.2.69) to (13.2.71) for small-signal linearized equations that (13.2.71) still holds for perturbation quantities:

$$\frac{D_1 p'}{Dt} = \frac{\gamma p_o}{\rho_o} \frac{D_1 \rho'}{Dt}. \tag{13.2.96}$$

Integration of this expression and use of (13.2.77) to define acoustic speed a_s yield

$$p' = a_s^2 \rho'. \tag{13.2.97}$$

Linearization of the conservation of momentum (13.2.86) yields

$$\rho_o \frac{\partial v_1'}{\partial t} = -\frac{\partial p'}{\partial x_1} - \frac{B_o}{\mu_0} \frac{\partial B_2'}{\partial x_1}. \tag{13.2.98}$$

In writing this equation, we have used (13.2.88) to eliminate J_3'.

The use of (13.2.97) to eliminate p' from (13.2.98) and the use of (13.2.95) to eliminate B_2' yield

$$\rho_o \frac{\partial v_1'}{\partial t} = \left(a_s^2 + \frac{B_o^2}{\mu_0 \rho_o}\right) \frac{\partial \rho'}{\partial x_1}. \tag{13.2.99}$$

The use of this expression and the linearized conservation of mass (13.2.94) to eliminate ρ' yields the single equation for v_1':

$$\frac{\partial^2 v_1'}{\partial t^2} = \left(a_s^2 + \frac{B_o^2}{\mu_0 \rho_o}\right)\frac{\partial^2 v_1'}{\partial x_1^2}. \tag{13.2.100}$$

Comparison of this result with (13.2.76) for ordinary acoustic waves shows that (13.2.100) describes longitudinal waves that propagate without dispersion with a propagation speed a given by

$$a = \left(a_s^2 + \frac{B_o^2}{\mu_0 \rho_o}\right)^{\frac{1}{2}}. \tag{13.2.101}$$

These waves are called magnetoacoustic waves and a is the magnetoacoustic velocity because the propagation speed is given by (13.2.101) as a combination of the acoustic velocity a_s and another velocity $\sqrt{B_o^2/\mu_0 \rho_o}$, which depends on magnetic flux density. This other velocity is numerically equal to the Alfvén velocity a_b obtained for transverse electromechanical waves and defined in (12.2.88).

Provided we replace a_s with a, as defined in (13.2.101), all the comments made about acoustic waves in the preceding section hold true for magnetoacoustic waves. Because of the bulk electromechanical coupling, it will be instructive to study the physical makeup of a magnetoacoustic wave. To provide a basis for comparison with ordinary acoustic waves we assume the same driving function we used for the acoustic wave example, namely, that the piston at $x_1 = 0$ is driven with small amplitude at angular frequency ω such that the gas velocity at $x_1 = 0$ is

$$v_1'(0, t) = V_m \cos \omega t. \tag{13.2.102}$$

The gas velocity at any point in the gas is then

$$v_1'(x_1, t) = V_m \cos\left(\omega t - \frac{\omega}{a} x_1\right). \tag{13.2.103}$$

This can be verified as the solution by seeing that the boundary condition (13.2.102) and the differential equation (13.2.100) are both satisfied. In addition, the infinite length in the x_1-direction results in no reflected waves traveling in the negative x_1-direction.

We now use the conservation of mass (13.2.94) and (13.2.95) to write

$$\frac{B_2'(x_1, t)}{B_o} = \frac{\rho'(x_1, t)}{\rho_o} = \frac{V_m}{a}\cos\left(\omega t - \frac{\omega}{a} x_1\right). \tag{13.2.104}$$

Finally, we use (13.2.88) to evaluate J_3:

$$J_3(x_1, t) = \frac{B_o \omega V_m}{\mu_0 a^2}\sin\left(\omega t - \frac{\omega}{a} x_1\right). \tag{13.2.105}$$
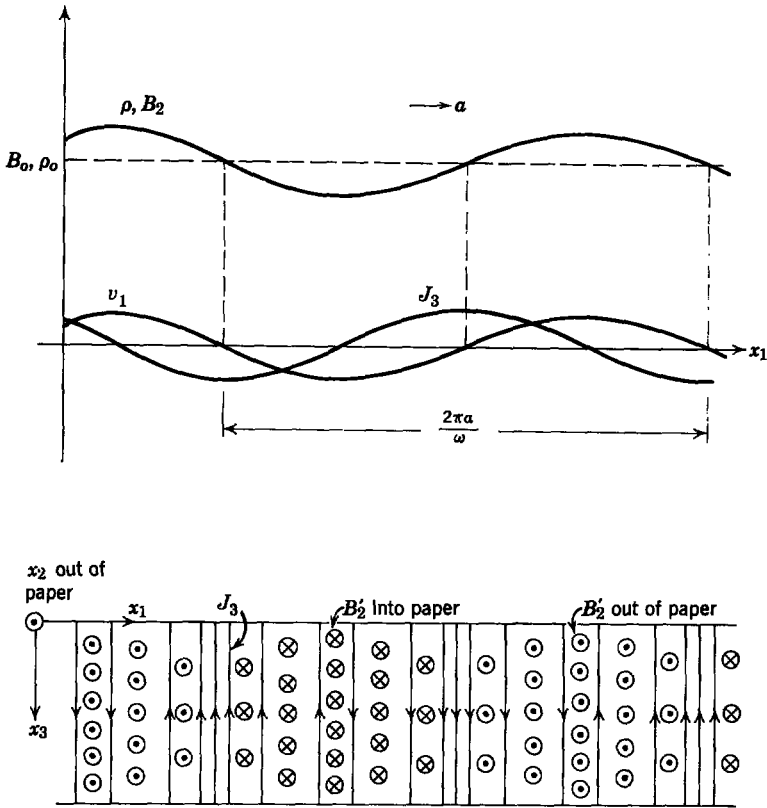
Fig. 13.2.13 Gas and electromagnetic variables in a magnetoacoustic wave of frequency ω propagating in the positive x_1-direction.

The variables described by (13.2.103) to (13.2.105) are illustrated for one instant of time in Fig. 13.2.13. As time passes, this pattern propagates with speed a in the positive x_1-direction. In describing J_3 the density of lines indicates the intensity of the current density, and for B_2' the density of the circles indicates the strength of the flux density. We already know that B_2' is excited by J_3. This can be verified by the right-hand rule or by (13.2.88). Also, as indicated by (13.2.95), the perturbation flux density and mass density are linearly related. Thus, when the gas is compressed, magnetic flux lines are compressed. This compression of flux lines induces a current density J_3, which interacts with the equilibrium flux density to produce a force that resists the compression. This makes the gas essentially less com- pressible, raises the effective continuum "spring constant," and makes the propagation velocity greater than the ordinary acoustic velocity.

It is clear from the pattern of current density in Fig. 13.2.13 why the highly conducting electrodes are necessary to close the current paths and maintain the one-dimensional nature of the problem.

In the example the waves were driven mechanically by a piston; they could have been driven equally well by local perturbations in flux density or current density. Furthermore, these waves can interact with an electric circuit that couples either to the flux density or to the current density. Thus magneto-acoustic waves provide the opportunity for continuum electromechanical coupling between a channel of highly conducting gas and an electric circuit.[*]

Although viscosity provides the loss mechanism that ultimately damps ordinary acoustic waves, magnetoacoustic waves are damped both by viscosity and by electrical losses that result from current flow in the presence of finite conductivity. In virtually all cases in which magnetoacoustic waves can be excited experimentally electrical losses predominate as the damping mechanism, and it is the limited electrical conductivity of gases that restricts the possibilities for practical utilization of magnetoacoustic waves for electro-mechanical coupling. This limitation is explored extensively in the literature.[†]

To illustrate the kinds of conditions necessary for the propagation of magnetoacoustic waves, we select conditions in which the waves have been excited and detected[‡]:

$$\text{Helium gas,} \qquad \rho_o = 0.0016 \text{ kg/m}^3,$$
$$B_o = 0.32 \text{ Wb/m}^2, \qquad T_o = 15{,}000°\text{K},$$
$$R = 2080 \text{ J/kg}°\text{K}, \qquad p_o = 0.5 \times 10^5 \text{ N/m}^2 \ (\tfrac{1}{2} \text{ atm}).$$
$$\gamma = 1.67,$$

The extremely high temperature is necessary to achieve high enough conductivity that will allow magnetoacoustic wave propagation without excessive damping. Needless to say, this was a pulsed experiment. From the data given the sound velocity is

$$a_s = \left(\frac{\gamma p_o}{\rho_o}\right)^{\!\!1/2} = 7240 \text{ m/sec.}$$

The Alfvén velocity is

$$a_b = \left(\frac{B_o^2}{\mu_0 \rho_o}\right)^{\!\!1/2} = 7150 \text{ m/sec.}$$

[*] H. A. Haus, "Alternating Current Generation with Moving Conducting Fluids," *J. Appl. Phys.*, **33**, 2161 (June 1962).

[†] G. L. Wilson and H. H. Woodson, "Excitation and Detection of Magnetoacoustic Waves in a Rotating Plasma Accelerator," *AIAA*, Vol. 5, No. 9, Sept. 1967, pp. 1633–1641.

[‡] Wilson and Woodson, *loc. cit.*

The magnetoacoustic velocity is

$$a = \sqrt{a_s{}^2 + a_b{}^2} = 10,200 \text{ m/sec}.$$

It is clear from these numerical values that in a gas a moderate flux density will yield a magnetoacoustic velocity that is considerably greater than the ordinary acoustic velocity; thus the electromechanical coupling in the wave is easily made strong.

Magnetoacoustic waves can also be excited in conducting liquids such as liquid metals; however, because of the high density of liquids it is difficult to obtain an Alfvén velocity large enough to affect appreciably the propagation velocity of longitudinal disturbances. It is easy to show that the propagation velocity of magnetoacoustic waves in conducting liquids is still given by

$$a = \sqrt{a_s{}^2 + a_b{}^2},$$

where a_s is the sound velocity given by (13.2.83) and a_b is the Alfvén velocity given by (12.2.88).

To determine how much the propagation velocity of a longitudinal disturbance can be affected in a conducting liquid by an applied magnetic field consider mercury for which the sound velocity and density are

$$a_s = 1410 \text{ m/sec},$$

$$\rho_o = 13,600 \text{ kg/m}^3.$$

The flux density necessary to give an Alfvén velocity that is 10 per cent of the sound velocity is

$$B_o = 18.5 \text{ Wb/m}^2.$$

This flux density (185,000 gauss) is obtainable at present only in large, high-field research magnets and it is a factor of 10 higher than obtainable with conventional iron-core electromagnets. A less dense liquid metal like sodium or potassium would require less flux density. For obtainable fields, however, the effect of a magnetic field is still small. Conducting gases, on the other hand, have low enough densities that the Alfvén velocity can be greater than the sound velocity at moderate flux densities, as we illustrated earlier.

In general, the propagation of disturbances in conducting fluids immersed in magnetic fields involves complex combinations of ordinary acoustic waves (longitudinal waves) and Alfvén waves (transverse waves) both propagating along magnetic field lines, and magnetoacoustic waves (longitudinal waves) propagating normal to magnetic field lines. These separate component waves couple through electromagnetic and gas variables

and are all damped by loss mechanisms. Thus the analysis of a disturbance, in general, is quite complex. Nonetheless, many phenomena can be understood in terms of the simple component waves we have studied separately.

13.3 DISCUSSION

In this chapter we have gone one step further in the analysis of electromechanical interactions between electrical systems and conducting fluids by using a compressible fluid model. The effects of compressibility on the basic conduction-type MHD machines were shown. Compressible fluids were shown to propagate longitudinal (acoustic) waves, and under appropriate conditions (long enough magnetic diffusion time) these waves can be modified significantly by the presence of a transverse magnetic field. Although the phenomena described and the techniques used in their analyses have important engineering applications, they were also intended to be indicative of the techniques available for the study of still other types of electromechanical interactions with fluids.

In Chapter 14 we introduce viscosity, another fluid-mechanical effect. We limit the discussion to incompressible fluids to highlight the principal effects of viscosity in MHD systems.

PROBLEMS

13.1. A static compressible fluid is subject to a gravitational force per unit volume $-\rho g$ (Fig. 13P.1). Under the assumption that the fluid has a constant temperature T_0 and that the fluid is a perfect gas so that $p = \rho RT$ find the distribution of density $\rho(x_1)$. The density at $x_1 = 0$ is ρ_0.
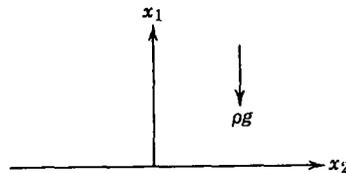
Fig. 13P.1

13.2. The MHD generator illustrated in Fig. 13P.2 uses a gas with constant specific heat capacities c_p and c_v and constant scalar conductivity σ. The dimensions are defined in the figure and it is assumed that the inlet values of all quantities are known. The loading factor K is to be held constant and the magnetic flux density is adjusted to satisfy the relation $B^2(z) A(z) = B_i^2 A_i$. For the constraint that the pressure be constant along the channel determine how the velocity v varies as a function of z.
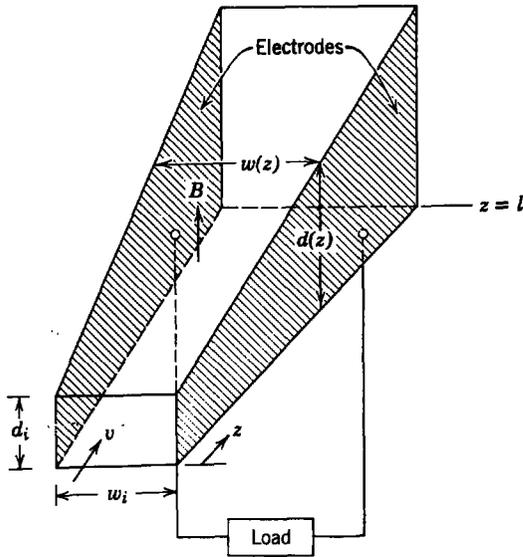
Fig. 13P.2

13.3. The dc MHD generator of Fig. 13P.3 has constant width w between the electrodes, and the magnetic flux density B_o is constant along the length of the channel. The gas is assumed ideal with constant specific heats and with constant electrical conductivity. The inlet quantities ρ_i, p_i, T_i, and v_i are assumed known. The electrodes are short circuited together.

  (a) Find the channel depth $d(z)$ necessary to maintain the temperature constant along the channel.

  (b) Find the mass density variation along the channel for the channel geometry found in part (a).

13.4. For the MHD generator of Fig. 13P.4 assume that all inlet quantities are known $(p_i, \rho_i, T_i, d_i, w_i, A_i)$ and that the working gas has constant, scalar conductivity σ and ratio of specific heats γ. We apply a magnetic flux density B_o, which is constant, over the length of the channel. We now specify that we wish to design a channel such that the loading factor K will be constant along the length of the channel.

  (a) For maintaining constant Mach number M along the channel find the following functions of z that satisfy the given conditions:

$$\frac{A(z)}{A_i}, \frac{d(z)}{d_i}, \frac{w(z)}{w_i}, \frac{v(z)}{v_i}, \frac{p(z)}{p_i}, \frac{T(z)}{T_i}.$$

  (b) Repeat part (a) for maintaining constant velocity v along the channel.

  (c) Assume that the given data is

$$\gamma = 1.4, \qquad \sigma = 40 \text{ mhos/m}, \quad R = 240 \text{ J/kg°K},$$
$$p_i = 5 \times 10^5 \text{ N/m}^2, \qquad \rho_i = 0.7 \text{ kg/m}^3, \qquad T_i = 3000°\text{K},$$
$$v_i = 700 \text{ m/sec}, \qquad w_i = 0.4 \text{ m} \qquad d_i = 0.2 \text{ m}.$$
$$K = 0.5, \qquad B_o = 4 \text{ Wb/m}^2$$

For the generators of parts (a) and (b) find the length of generator necessary to reduce the total enthalpy per unit mass $(c_p T + \frac{1}{2}v^2)$ by 10%.
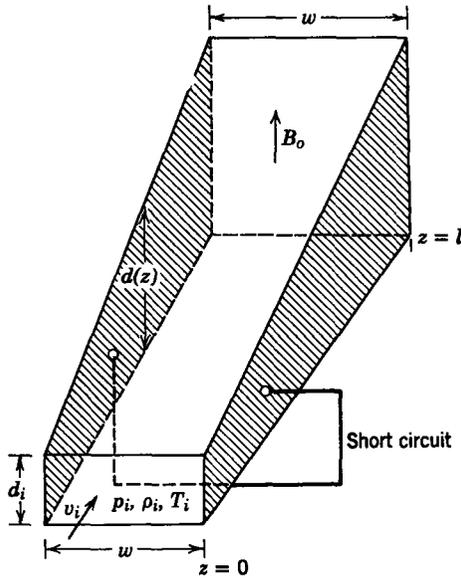
Fig. 13P.3
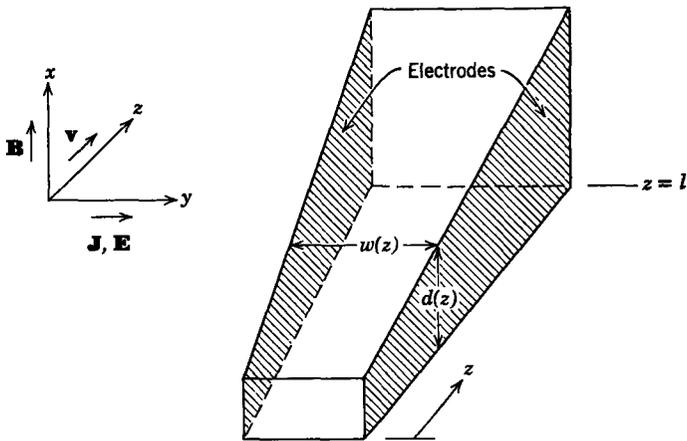
Fig. 13P.4

13.5. An MHD generator (Fig. 13P.4) uses an ideal gas with a constant ratio of specific heats $\gamma = 1.4$ and a constant, scalar, electrical conductivity $\sigma = 50$ mhos/m. At the inlet to the MHD generator channel the parameters and variables are adjusted to have the values

$$B_i = 4 \text{ Wb/m}^2, \qquad v_i = 700 \text{ m/sec},$$
$$\rho_i = 0.7 \text{ kg/m}^3, \qquad M_i^2 = 0.5,$$
$$p_i = 5 \times 10^5 \text{ N/m}^2, \qquad d_i = 0.5 \text{ m}$$
$$w_i = 1 \text{ m},$$

The aspect ratio of the channel is to remain constant so that the electric and magnetic fields will vary as

$$\frac{B(z)}{B_i} = \frac{E(z)}{E_i} = \left[\frac{w(z)}{w_i}\right]^{-1} = \left[\frac{d(z)}{d_i}\right]^{-1} = \left[\frac{A(z)}{A_i}\right]^{-\frac{1}{2}},$$

where A is the channel cross sectional area. For the conditions specified and for a loading factor $K = 0.5$ complete the following:

(a) Find the area as a function of z necessary to keep the gas velocity constant.
(b) For the channel of part (a) specify the length l necessary to reduce the gas temperature by 20 percent; that is, find l such that $T(l)/T_i = 0.8$.
(c) Calculate and plot curves of $p(z)$, $\rho(z)$, $T(z)$ and $M^2(z)$ over the length of the channel.
(d) Calculate the total electrical power drawn from this generator under the conditions given.

13.6. An ion propulsion device is represented schematically in Fig. 13P.6. The lateral dimensions are much larger than the separation of the accelerator electrodes so that fringing fields can be neglected. Ions, each having a charge q and mass m are injected with negligible initial velocity at $x = 0$. The system operates in the steady state in the space-charge-limited mode, in which case the solution for the electric field between the electrodes is

$$\mathbf{E} = \mathbf{i}_x \frac{4}{3} \frac{V_o}{L^{4/3}} x^{1/3},$$

and the solution for the charge density between the electrodes is

$$\rho_e = \frac{4}{9} \frac{\epsilon_0 V_o}{L^{4/3} x^{2/3}}$$

The charge on each ion does not change during the acceleration process; that is,

$$\frac{\rho_e}{\rho_m} = \frac{q}{m},$$
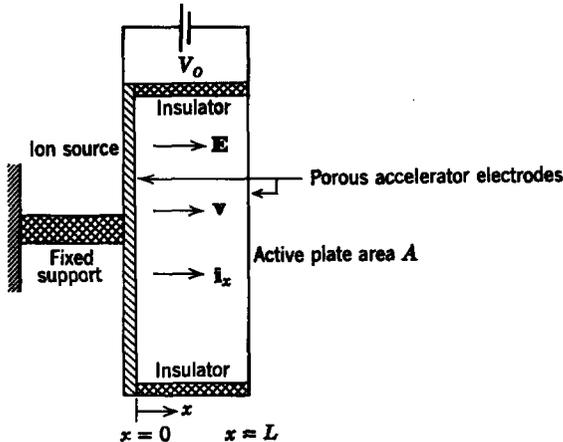
Fig. 13P.6

where ρ_m is mass density. The pressure in the ion gas is negligibly small. For steady-state operation complete the following:

  (a) Find the velocity of the ion gas as a function of x between the electrodes.
  (b) Find the magnitude and direction of the force that must be supplied by the fixed support to keep the accelerator system at rest.

13.7. In Fig. 13P.7 a liquid is placed between rigid walls and a movable piston. The liquid has a speed of sound a. The system is uniform in the x_2- and x_3-directions ($\partial/\partial x_2 = \partial/\partial x_3 = 0$). Assuming that the piston is moved by a velocity source $V = V_o \cos \omega t$ at $x_1 = -L$,
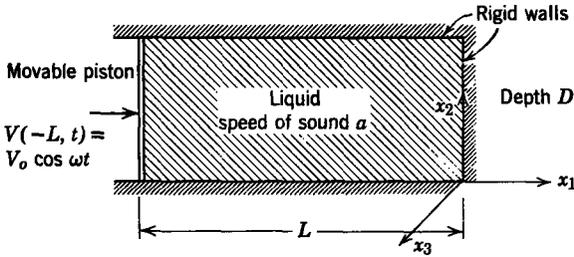
Fig. 13P.7

complete the following:

  (a) Find the pressure in the liquid at $x_1 = -L$. Take the equilibrium pressure inside and outside the liquid as p_o.
  (b) At what frequencies will there be resonances in the pressure, $p(-L, t)$?

13.8. A perfectly conducting compressible inviscid fluid fills the region $0 < x_2 < d$ as shown in Fig. 13P.8. When the fluid is static, it is permeated by a magnetic field $\mathbf{H} = H_o \mathbf{i}_3$. The fluid is set in motion by a piston at $x_1 = -L$ having velocity as shown, and is constrained at $x_1 = 0$ by a piston having mass M.

  (a) *Derive* a differential equation (one equation in one unknown) for the velocity $v_1(x_1, t)$. Use a linearized analysis.
  (b) Find the velocity of the piston, which in equilibrium is at $x_1 = 0$, under the conditions shown in Fig. 13P.8.
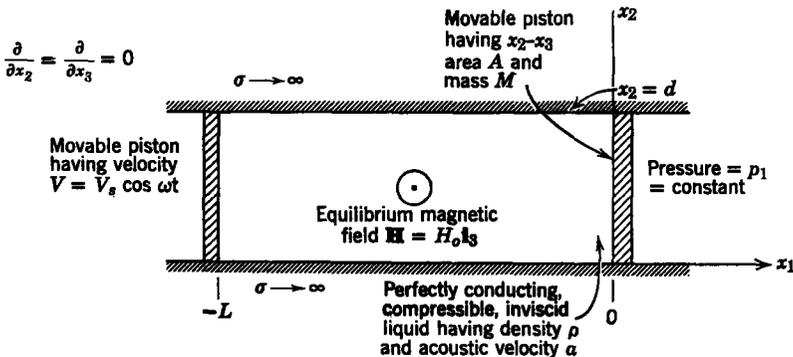
Fig. 13P.8
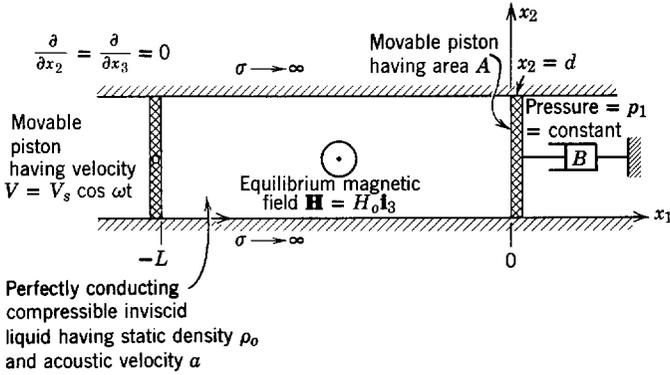
Fig. 13P.9

13.9. The region $0 < x_2 < d$ in Fig. 13P.9 is filled with a perfectly conducting inviscid compressible fluid. When the fluid is static, it is permeated by a magnetic field $H = H_o i_3$. The fluid is excited by a piston at $x_1 = -L$ with velocity $v(t)$, as shown, and constrained at $x_1 = 0$ by a movable massless insulating piston connected to a dashpot.

(a) *Derive* a differential equation (one equation in one unknown) for the velocity $v_1(x_1, t)$. Use a linearized analysis.

(b) The system is to be used as a delay line in which the object is to delay a signal by a fixed time without distorting the signal. If the signal is to be transmitted delayed and undistorted to $x_1 = 0$, the backward traveling wave must be eliminated by choosing a specific value for the dashpot coefficient B. Find this value in terms of the appropriate constants of the system.

13.10. The system shown in Fig. 13P.10 consists of a cylinder of cross-sectional area A_c containing a liquid of compressibility κ and equilibrium density ρ_l at equilibrium pressure p_o. The fluid is constrained at $x = 0$ by the closed end of the cylinder and at the other end by a rigid piston of mass M and thickness Δ. The equilibrium length of the liquid in the x-direction is L_1. The left face of the piston is connected to a thin elastic rod of cross-sectional area A_s, modulus of elasticity E, and equilibrium density ρ_s. The equilibrium length of the elastic rod is L_2. The left end of the elastic rod is driven by a stress source $T_o + T_s(t)$, where $T_s(t) \ll T_o$. For small-signal dynamic operation around an equilibrium point the general solutions are for the elastic rod: $-(L_1 + L_2 + \Delta) < x < -(L_1 + \Delta)$, $T(x, t)$ and $v_e(x, t)$; for the fluid $-L_1 < x < 0$, $p(x, t)$ and $v_l(x, t)$. Assume that except for constants to be determined by boundary conditions these solutions are known. Set up the equations that describe all the boundary conditions necessary for specializing constants in the general solutions. *Note.* You are not required to solve these equations.
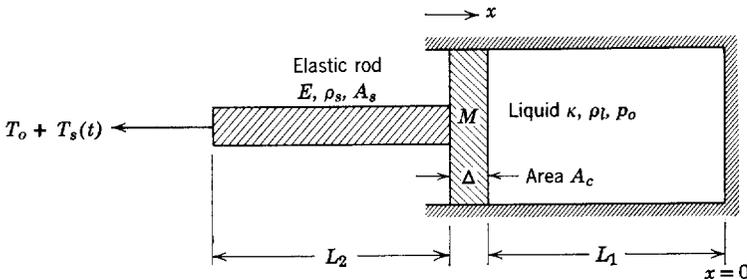
Fig. 13P.10

13.11. A slightly compressible inviscid fluid flows with a steady velocity V_o in the x-direction (Fig. 13P.11). The motions are in the x-direction and only a function of (x, t). The velocity of sound in the fluid is a_s.

  (a) Find the dispersion equation for small disturbances in the form of $p = \text{Re}$ $[\hat{p}e^{j(\omega t - kx)}]$.

  (b) Under what condition will the phases of both waves propagate in the positive x-direction?

Sound velocity = a_s

$\longrightarrow x$

$\longrightarrow V_o$
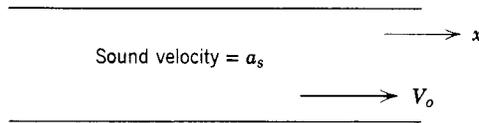
Fig. 13P.11

13.12. A static, inviscid fluid of conductivity σ is immersed in a uniform magnetic field H_o (Fig. 13P.12). In the limit in which $\sigma \to \infty$, it is possible for magnetoacoustic plane waves to propagate along the x-axis. In this problem investigate the consequences of having a finite conductivity σ.

y

$H_o \quad \dfrac{\partial}{\partial y} = \dfrac{\partial}{\partial z} = 0$

x

z
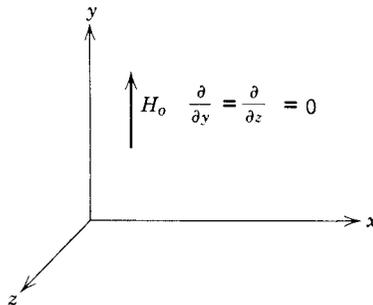
Fig. 13P.12

  (a) Write the linearized equations of motion for perturbations that are compressional (along the x-axis) and depend only on (x, t). (You need not combine these equations.)

  (b) Consider solutions of the form $v_x = \text{Re}\,[\hat{v}e^{j(\omega t - kx)}]$ and find the dispersion relation between ω and k. Show that in the limit $\sigma \to \infty$ the lossless dispersion equation is retained.

  (c) Show that when σ is small there are two pairs of waves, each pair consisting of a forward and backward traveling wave. What would you call these waves?

  (d) Consider the case in which σ is very large but finite (slight losses) and in which the excitation is sinusoidal (ω is real). Find an approximate expression for the rate at which waves decay in space. *Hint.* Write the dispersion equation in the form

$$k^2 = \frac{\omega^2}{a^2} - j\,\frac{f(\omega, k)}{\sigma},$$

where a is the phase velocity of magnetoacoustic waves. When σ is large but finite, the second term can be approximated by making $k^2 \approx (\omega^2/a^2)$. (Why?)